Revista Brasileira de Ensino de Física, vol. 42, e20190283 (2020)
www.scielo.br/rbef
DOI: http://dx.doi.org/10.1590/1806-9126-RBEF-2019-0283

Didactic Resources

Teaching wave-particle complementarity using the Virtual Mach-Zehnder Interferometer

C J H Cavalcanti*[1], F Ostermann[1], J S Netto[2], N W Lima[1]

[1]Universidade Federal do Rio Grande do Sul, Departamento de Física, Instituto de Física, Porto Alegre, RS, Brasil
[2]Instituto Federal do Rio Grande do Sul, Bento Gonçalves, RS, Brasil

Received on October 11, 2019; Revised on December 31, 2019; Accepted on January 4, 2020.

We propose the teaching of wave-particle duality mediated by a software called Virtual Mach-Zehnder Interferometer, developed by our research group. We introduce the Dirac's formalism contextualized on the Mach-Zehnder Interferometer, constructing explicitly the operators that represent the action of each device on the interferometer, calculating probability amplitudes on screens. Wave-particle complementarity is explored both in the qualitative and quantitative perspective, using computational simulations provided by the software. By studying concepts such as visibility, predictability and distinguishability, we explore the intermediate interference patterns aiming to expand what has not traditionally been found in textbooks and most courses. With the purpose of illustrating the application of the software in the classroom, the paper presents some didactical situations experienced by students of a physics teacher-training course during a quantum physics class, discussing students' discursive interactions. The didactical approach to quantum interference phenomena carried out with the software, whether qualitative or quantitative, can promote rich and interesting discussions among students, exploring recent topics of quantum physics and allowing them to have a deeper and articulated understanding of the theory.
Keywords: Mach-Zehnder interferometer, Quantum Physics teaching, Complementarity Principle.

1. Introduction

The main purpose of this paper is to take an additional step towards a comprehensive presentation of the Mach-Zehnder Interferometer (MZI), revisiting the discussion on interference phenomena carried out in our previous work [1], supported by the same software – the Virtual Mach-Zehnder Interferometer (VMZI). The additional step consists in moving from classical to quantum interference phenomena, in order to address important fundamental concepts of quantum physics, not quantitatively addressed in our previous works. Although the interference patterns are mathematically "similar" in both contexts, there are crucial theoretical differences concerning the explanations about formation or destruction of these patterns on classical and quantum descriptions. To make clear these differences, some key concepts will be introduced along this paper, specially how to (re)interpret the visibility in the context of quantum interference and its relation with *path distinguishability*. This topic is important to understand the complementarity between wave and particle behavior of quantum objects in a quantitative framework, and, chiefly, to resignify Complementarity Principle in the case of *intermediary phenomena*, which was not originally addressed by Bohr.

It is known that the concepts involved in quantum interference are complicated to teach and students show difficulties to understand them. Wave-particle duality is a central issue on quantum interference and it is usually poorly understood by the students. The Mach-Zehnder setup can be valuable in such contexts, since it *a priori* avoids usual arguments employed by some students, who conceive the genesis of quantum interference process on the double-slit system as if it were a deflection of a classical particle by the slits [2]. Similar classical reasoning about quantum objects also appears in studies dealing with quantum tunneling [3]. These difficulties rely on students' troubles on reconcile quantum and classical concepts [4], which usually arise when they face didactical activities on quantum interference.

Several works have been developed to investigate student learning on these topics, from which valuable didactical resources were developed. It is worth to mention the interactive tutorials based on students' difficulties, developed by Singh [5]; the exploratory tutorial via simulation of Stern-Gerlach experiment, developed by Zhu and Singh [6]; the collection of interactive animations and visualizations for teaching quantum physics, aiming insertion at all levels of the undergraduate curriculum, developed by Kohnle, *et al.* [7] or the Institute of Physics New Quantum Curriculum, developed by Kohnle, *et al.* [8], which consists in a collection of freely available online materials for a first university course quantum mechanics based on two-level systems. The MZI appears in a considerable part of literature concerning to quantum physics teaching and its quantum description is detailed in some of them [9, 10, 11, 12, 13]. Our group has also

*Correspondence email address: claudio.cavalcanti@ufrgs.br.

produced some papers adopting the MZI as the central device and didactical tool over the past years [1, 14, 15, 16, 17, 18, 19, 20, 21, 22], two of them addressing complementarity [23, 24]. In this paper, the mathematical treatment, barely explained in previous papers, will be much better detailed.

This paper is divided into two main parts: in part I we present the basic features of MZI and also the physics needed to understand the quantum description of quantum interference phenomena. We also develop a basic version of quantitative complementarity, accessible for undergraduate and graduate students. To do so, we detail the quantum description in a contextualized way, putting efforts including the most basic version of quantitative complementarity, which can be carried out allowing the reflection coefficients of the beam-splitters freely assuming any value between 0 and 1. Simply by varying these parameters we increase availability of path information (this concept will be better explained in section 2.3.5), decreasing the visibility of the interference pattern. There are multiple ways to obtain path information on the MZI (using polarization filters or non-demolition detectors), but we will restrict our discussion to the more basic way, based only on the variability of reflection coefficients of the beam splitters.

In part II, we will present the analysis of some teaching activities with the software VMZI[1], discussing students' discursive interactions. Considering that computational simulations can lead to positive effects on science learning [see the revision in 25], we adopted this computational resource in a pedagogically articulated design, in which there is an interplay with pre-designed classes, activities and assistance of a teacher. In addition, we used a study based on small groups, to better engage students in an active way without lose concentration on focused topics [26].

[1]The software can be downloaded from the following link: http://www.lief.if.ufrgs.br/~cjhc/vmzi.html. The link provided in our previous paper [1] is not active anymore.

2. Part I: The Physics

2.1. The Mach-Zehnder Interferometer: basic issues

In order to make this paper self-contained, we repeat the description of basic issues of MZI as we did in our previous work [1], but modified to deal with the quantum case. In MZI, interference emerges due to its two-way character obtained from a combination of mirrors and beam splitters, as shown in Figure 1 [1, 18, 27, 28]. We assume (1) the beam splitters are symmetric, like a cubic beam splitter [29, p. 183], i.e. the beam-splitter properties are the same, regardless the input port from where the incident beam comes from; (2) they are lossless, i.e. do not absorb energy of incident wave (do not absorb photons) and (3) they are non-polarizing, i.e. do not change the photon polarization state. They can be unbalanced, i.e. they may have different values of reflection and transmission coefficients (the sum of these two parameters must be equal to one). In the quantum mode it is better to define R_1 and T_1, respectively, as the reflection and

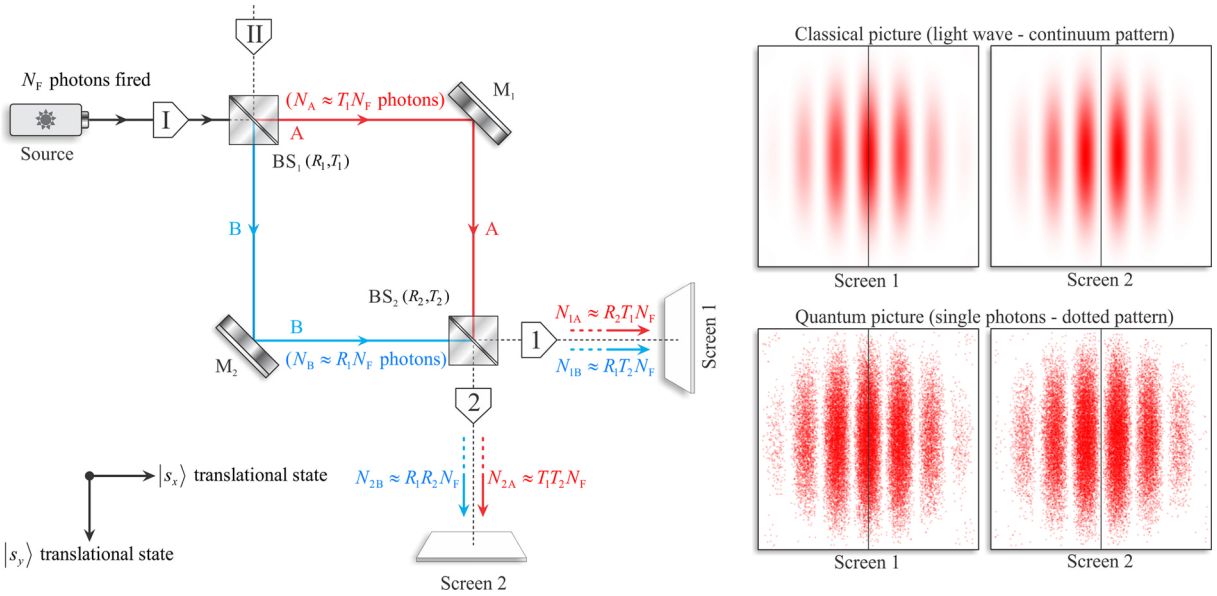

Figure 1: Mach-Zehnder interferometer with symmetric unbalanced cubic beam splitters BS_1 and BS_2, with reflection (transmission) coefficients R_1 ($T_1 = 1 - R_1$) and R_2 ($T_2 = 1 - R_2$), respectively. Two input ports (I and II) and two output ports (1 and 2) are available. A light source is placed at input port I and screens are placed at the output ports 1 and 2 to observe the interference patterns. Examples of interference patterns is shown at right, for classical and quantum cases (considering balanced beam splitters, i.e. $R_1 = R_2 = T_1 = T_2 = 0.50$). The vertical line in the centre of each screen is an aid to visualize that interference pattern on screen 1 is inverted related to pattern on screen 2. Quantities N_A, N_B, N_{1A}, N_{2A}, N_{1B} and N_{2B} will be explained in latter sections.

 DOI: http://dx.doi.org/10.1590/1806-9126-RBEF-2019-0283

transmission *probabilities*, as we will explain in section 2.2.

Figure 1 shows a schematic view of MZI. In the quantum picture, the source, placed at the input port I, emits a beam with extremely small intensity, namely, one photon at a time (monophotonic pulse). The first experimental verification of interference at single photon level was reported in the study of Pfleegor and Mandel [30]. Later, in 1985, the first source of monophotonic pulses was developed by Alain Aspect and Philippe Grangier[2]. Since then, their research group produced several important papers focused on foundations of quantum physics. One of them studied the single photon interference using the MZI [31]. Single photon sources are still a remarkable research topic and have been undergoing significant improvements [32]. An incident photon entering by input port I interacts with each device on the interferometer (beam splitters, mirrors and so on). Each device transforms the initial translational state of the photon in a way that a pattern will gradually arise on each screen – these patterns will exhibit interference or not, depending on the parameters R_1 and R_2 (this will be detailed on section 2.2).

It is worth to stress that the form of interference pattern depends strongly on the interferometer configuration. If the mirrors and beam splitters are properly aligned and the length of the arms A and B are different, a circular pattern can be obtained in each screen. If we place a convergent lens in one of the arms [27], similar circular patterns can be obtained (setting equal lengths for each arm and aligning the mirrors and beam-splitter's coating film at 45 degrees). A third possible configuration can be obtained aligning the mirrors at angles slightly different from 45 degrees [33, p. 86]. In this configuration, it is not difficult to show that MZI reduces to two double slit systems [1], each consisting of two virtual coherent sources (one system for each screen). The virtual sources related to screen 1 are in phase and the sources related to screen 2 have a π phase difference between themselves. Hence, the resulting patterns are like that obtained in the double slit experiment (Young's interference), as shown in Figure 1. Because this class of pattern is most familiar to the students, we choose this configuration in this version of Virtual Mach-Zehnder Interferometer (VMZI). Moreover, the calculation and visualization of interference patterns in VMZI considers the finite size of aperture of the light source (circular aperture). Thus, the Airy function [34, p. 469, 35] modulates the interference patterns on the screens, as shown in Figure 1. As done in our previous work, we will focus the mathematical analysis on the interference phenomena and, for didactical purposes, will not explicitly address quantum diffraction effects here.

[2] Conference available on YouTube (http://www.youtube.com/watch?v=Cg7jMXQHxvM). Full transcription (and same conference video) is available in https://www.falling-walls.com/videos/Alain-Aspect–1216.

2.2. Quantum picture of Mach-Zehnder Interferometer: single photon interference

In quantum picture of the MZI, we consider that the source emits one photon at a time. Each photon interacts with beam splitters and mirrors until it finally hits the screens, producing a punctual mark, building interference patterns photon-by-photon[3]. As stated by Dirac [36, p. 7], each photon "is located somewhere in the region of space through which the beam is passing and has a momentum in the direction of the beam". First, we pay special attention to the word *beam*: in classical picture, the laser beam splits into two beams A and B in the interferometer – in quantum picture, when a single photon enters the interferometer at a time, the word *beam* can be thought as the possible paths A and B for the photon in MZI. Furthermore, the word *location* cannot be confused with *position*: the photon position is undefined, since it is unlocalizable (in the classical sense) in any of the beams (A or B) – even if only a single beam is available (e.g. removing the first beam splitter) the exact position of the photon in the beam is *a priori* undefined. The photon *location* in MZI, or in which beam the photon is, can only be unveiled by a measurement process (e.g. placing a photon detector in one of the arms). Dirac [36, p. 7] also states that "when we have such information about the location and momentum of a photon, we shall say that it is in a definite translational state". Two possible quantum translational states[4] in the interferometer ($|s_x\rangle$ and $|s_y\rangle$) are shown in Figure 1. These names were chosen in analogy to the possible propagation directions in the interferometer. These both states are orthogonal, i.e., $\langle s_x \mid s_y\rangle = 0$, defining a complete basis in a two-dimensional Hilbert vector space – in this case the *closure relation* $\hat{\mathbf{I}}_{\mathrm{T}} = |s_x\rangle\langle s_x| + |s_y\rangle\langle s_y|$ holds.

Photons are not classical particles and we must avoid to directly assign classical trajectories to them. When one says that the photon has a definite translational state $|s_x\rangle$ this does not mean that a photon travels in a straight line along the x-direction in a definite arm of interferometer. This translational state can be described as a continuous linear quantum superposition of momentum states with an angular distribution around x-direction (supposing a narrow quantum beam of photons of definite frequency – not a perfectly collimated beam). For $|s_y\rangle$ the reasoning is the same, but the momenta is distributed around y-direction such that $|s_x\rangle$ and $|s_y\rangle$ states are fully distinguishable to each other and, consequently, $\langle s_x \mid s_y\rangle = 0$. Despite being common to find, even in

[3] Dirac [36] defined this as *self-interference*.

[4] We chose to mathematically describe the x-translational state by $|s_x\rangle$ instead $|x\rangle$, to avoid confusion with x-position eigenstates, usually expressed by the later. The same choice was made regarding y-translational state. In this paper we will not present the foundations of Dirac's formalism – the following sections were conceived considering some prior knowledge about this topic. For an introduction to Dirac's formalism, we recommend the following references (in increasing order of complexity): Michelini, *et al.* [37], Auletta, *et al.* [38, chapters 2 and 3], Auletta, *et al.* [39, chapters 1 and 2] and Jammer [40, chapter 1].

specialized literature, utterances like "go along a single path" [41, p. 052109], or "path taken by a particular quantum [object]" [42, p. 4285] referring to quantum objects, it can be a misleading idea to assign classical trajectories to photons. What these authors had in mind was not to assign a classical trajectory to photons[5]. They were probably referring to a more sophisticated definition of trajectory adopted by Kwiat [49], associating the "photon trajectory" inside the MZI with the "existence of any which-way information, labelling which path a photon took" [49, p. 429]. As argued by Englert, *et al.* [45], "statements about the actual path through the interferometer are meaningful only if they represent path knowledge acquired by a suitable observation". This path information reduces the visibility of interference pattern, as will be explained in section 2.3. In theory, the property *path* is closely related to the knowledge about the quantum translational state of the photon inside the interferometer. After the photon interacts with first beam splitter, there are only two possible outcomes: total reflection or total transmission of the photon – it is known that a single photon does not "breaks up" into two "half-photons" when it interacts with beam splitters [31, 50]. These two outcomes are probabilistic and mutually exclusive: in quantum picture of MZI, R_1 (R_2) and $T_1 = 1 - R_1$ ($T_2 = 1 - R_2$) are, respectively, the photon reflection and transmission probabilities, considering the first (second) beam splitter. On transmission, the translational state remains $|s_x\rangle$, on reflection it is changed to $|s_y\rangle$.

Due to the impossibility of assignment of classical trajectories to photons, we will use here the word *associated*. Unlike classical particles, they can be in a translational state that is not simply defined by $|s_x\rangle$ or $|s_y\rangle$, but in a linear superposition of both (mathematically, in a *linear combination* of both). Thus, in this case the quantum translational state of the photon can be *associated* with the two possible paths A and B. After the photon's interaction with first beam splitter, its initial quantum translational state $|s_x\rangle$ is transformed into a superposition described by $t_1 |s_x\rangle + r_1 |s_y\rangle$, i.e., a quantum state which has two quantum translational characteristics at once. The r_1 and t_1 parameters are, respectively, the probability amplitudes of photon being reflected and transmitted by first beam splitter (they are complex numbers). To understand this in a more precise framework, we need to describe in detail the evolution of the photon's translational state inside the interferometer. To do this, we must consider the action of each device on the interferometer as mathematically represented by a linear quantum operator. This will be explained in the following sections.

[5] This consideration depends on which interpretation is adopted. If one adopts an interpretation of quantum phenomenon that assigns a corpuscular ontology for the photon, trajectories could apparently be a reasonable argument. In this paper we focus on the Copenhagen interpretation, which assigns a dualist ontology for quantum objects (photons in the present case). The possibility of assigning or not trajectories to the photons which propagate inside the interferometer is still a matter of debate today, but these trajectories are not strictly classical. See for example the works of Danan, *et al.* [43], Duprey and Matzkin [44], Englert, *et al.* [45], Saldanha [46], Sokolovski [47], Vaidman [48], among others.

2.2.1. The quantum operator representing the action of the beam splitter

Defining $\hat{\mathbf{S}}_1$ as the operator that represents the action of first beam splitter on the translational state of the incident photon, our first task is to write it explicitly. Obviously, it should include the reflection and transmission as the only two possible outcomes of the interaction between the photon and the first beam splitter. Since the incident photon can come from two input ports (I or II), this fact must be considered as well. To help to understand the construction of the mathematical form of this operator, we propose the following statements:

1. When the incident photon comes from input port I and interacts with the first beam splitter with a reflection probability equal to R_1 and transmission probability equal to T_1, the part of the operator $\hat{\mathbf{S}}$ which describes this interaction is $r_1|s_y s_x| + t_1 |s_x\rangle \langle s_x|$. Since we have $(r_1|s_y\rangle\langle s_x| + t_1 |s_x\rangle \langle s_x|) |s_x\rangle = t_1 |s_x\rangle + r_1|s_y\rangle$, this means that reflection flips photon's translational state from $|s_x\rangle$ to $|s_y\rangle$ and transmission keeps it unchanged and described by state vector $|s_x\rangle$.
2. When the photon comes from the input port II, the interaction with the first beam splitter will be described by $r_1^{'} |s_x\rangle \langle s_y| + t_1^{'}|s_y\rangle\langle s_y|$. Thus, $\left(r_1^{'} |s_x\rangle \langle s_y| + t_1^{'}|s_y\rangle\langle s_y|\right) |s_y\rangle = r_1^{'} |s_x\rangle + t_1^{'}|s_y\rangle$. In this case the reflection flips the photon's translational state from $|s_y\rangle$ to $|s_x\rangle$ and transmission keeps its translational state unaltered and described by the state vector $|s_y\rangle$. If the beam splitter is not symmetric, we must consider $r_1^{'} \neq r_1$ and $t_1^{'} \neq t_1$. Here, we will consider both beam splitters as symmetric.

To account these two statements, the operator $\hat{\mathbf{S}}_1$ can be written as follows:

$$\begin{aligned} \hat{\mathbf{S}}_1 &= r_1 \left(|s_y\rangle\langle s_x| + |s_x\rangle\langle s_y|\right) \\ &+ t_1 \left(|s_x\rangle \langle s_x| + |s_y\rangle\langle s_y|\right) \\ &= r_1 \left(|s_y\rangle\langle s_x| + |s_x\rangle\langle s_y|\right) + t_1 \hat{\mathbf{I}}_{\mathrm{T}}. \end{aligned} \tag{1}$$

This mathematical form holds true only for a symmetric and lossless beam splitter. Let us show the action of the beam splitter, quantum mechanically described by the operator $\hat{\mathbf{S}}_1$, on the translational state of the photon when it enters in the interferometer by input ports I or II. If the photon comes from input port I (II) its initial state is $|s_x\rangle$ ($|s_y\rangle$) state. So, it is easy to show that the translational state $\left|\Psi^{\mathrm{I}}_{\mathrm{BS}_1}\right\rangle$ ($\left|\Psi^{\mathrm{II}}_{\mathrm{BS}_1}\right\rangle$) of the photon coming from input port I (II), after its interaction with the first beam splitter, is

$$\left|\Psi^{\mathrm{I}}_{\mathrm{BS}_1}\right\rangle = \hat{\mathbf{S}}_1 |s_x\rangle = r_1|s_y\rangle + t_1 |s_x\rangle , \tag{2}$$

 DOI: http://dx.doi.org/10.1590/1806-9126-RBEF-2019-0283

for a photon coming from input port I, and

$$\left|\Psi^{\mathrm{II}}_{\mathrm{BS}_1}\right\rangle = \hat{\mathbf{S}}_1|s_y\rangle = r_1\,|s_x\rangle + t_1|s_y\rangle \tag{3}$$

for a photon coming from input port II. Considering the situation shown in Figure 1, the initial translational state is transformed according to (2) and has the translational character $|s_x\rangle$ (related to transmission – a quantum translational characteristic *associated* with the path A) and $|s_y\rangle$ (related to reflection – a quantum translational characteristic *associated* with the path B). This results in a counterintuitive conclusion: after the interaction with the first beam splitter, the photon translational state is associated with two paths A and B at once (with unequal probabilities $|t_1|^2 = t_1 t_1^* = T_1$ and $|r_1|^2 = r_1 r_1^* = R_1$, respectively – the asterisk denotes the complex conjugate). In other words, the photon is not localizable in one definite arm. If an ideal detector is placed in arm A, for example, and a measurement is performed in each incident photon, a state reduction takes place (as stated by Copenhagen Interpretation). In this case, definite results $|s_x\rangle$ (detector triggers – path A), with probability T_1, or $|s_y\rangle$ (detector does not triggers – path B), with probability R_1 will be obtained [51], producing a sequence of possible outcomes $|s_x\rangle$ (associated with A) or $|s_y\rangle$ (associated with B). The approximate number of occurrences of each one is proportional to their respective probabilities T_1 and R_1. If no measurement is performed, its translational state remains indefinite respective to both possible translational characteristics (if $R_1T_1 \neq$). So, the translational state of the photon after its interaction with first beam splitter acquires two translational characteristics and can be *associated* both to the path A (with probability R_1) and path B (with probability T_1). Is the first beam splitter which prepares the photon in a quantum superposition, leading to interference in conjunction with the second beam splitter (in fact, the first beam splitter alone is not enough to accomplish interference – the second one plays an important role too, as we will see later). As this superposition of translational states is assigned to each single photon in the interferometer, the denomination *self-interference* is commonly used to highlight the distinction from classical interference of light, in which the superposition involves two explicit beams of light. In the next sections, we will return to single photon interference and see that the role of unbalance on beam splitters results in available path information, reducing (or even vanishing) the contrast of interference pattern. This is the essence of the quantitative version of *complementarity principle*

An important property of $\hat{\mathbf{S}}_1$ operator can be deduced from conservation of probability. Since the beam splitters are known to be lossless by hypothesis, no photon absorption happens and the relation $R_1 + T_1 = 1$ holds true. This is, in essence, the conservation of energy by means of conservation of total number of photons N_{F} fired by the source (see Figure 1 – subscript F means *fired*). If two ideal and 100 percent efficient photon detectors were placed one in each arm of the interferometer, the detector in A would register $N_{\mathrm{A}} \approx T_1 N_{\mathrm{F}}$ transmitted photons (i.e., associated to path A) and the detector in B would register the remaining $N_{\mathrm{B}} \approx R_1 N_{\mathrm{F}}$ reflected photons (i.e., associated to path B). Since the reflection and transmission are probabilistic events, the quantities N_{A} and N_{B} are not exactly equal to $T_1 N_{\mathrm{F}}$ and $R_1 N_{\mathrm{F}}$, respectively. However, if the beam splitter is lossless, their sum equals to N_{F} ($N_{\mathrm{A}} + N_{\mathrm{B}} = N_{\mathrm{F}}$). To account this phenomenon, the operator $\hat{\mathbf{S}}_1$ must be *unitary*. This is mathematically expressed by the condition $\hat{\mathbf{S}}_1^\dagger \hat{\mathbf{S}}_1 = \hat{\mathbf{I}}_{\mathrm{T}}$ ($\hat{\mathbf{S}}_1^\dagger = r_1^*\left(|s_x\rangle\langle s_y| + |s_y\rangle\langle s_x|\right) + t_1^* \hat{\mathbf{I}}_{\mathrm{T}}$ is the adjoint operator of $\hat{\mathbf{S}}_1$). It is straight forward to show that this unitarity condition leads to $(r_1^* t_1 + r_1 t_1^*)\left(|s_x\rangle\langle s_y| + |s_y\rangle\langle s_x|\right) + (R_1 + T_1)\,\hat{\mathbf{I}}_{\mathrm{T}} = \hat{\mathbf{I}}_{\mathrm{T}}$. Consequently, we obtain two conditions: $R_1 + T_1 = 1$ (which means that probability is conserved) and $r_1^* t_1 + r_1 t_1^* = 0$.

The second condition can be physically interpreted as follows: if r_1 and t_1 are written in complex polar form, $r_1 = \sqrt{r_1^* r_1}\mathrm{e}^{\mathrm{i}\delta_r} = \sqrt{R_1}\mathrm{e}^{\mathrm{i}\delta_r}$ and, analogously, $t_1 = \sqrt{T_1}\mathrm{e}^{\mathrm{i}\delta_t}$. The quantities δ_r and δ_t are, respectively, the phases of reflected and transmitted photon. The condition $r_1^* t_1 + r_1 t_1^* = 0$ leads directly to a simple relation between these phases:

$$\delta_r - \delta_t = \frac{\pi}{2}. \tag{4}$$

In other words, the phase difference between the reflected and transmitted photon by a symmetric beam splitter is $\pi/2$. This same result was classically obtained by Degiorgio [52] as a consequence of the energy conservation of the wave when it interacts with a symmetric and lossless beam splitter. The same result given by (4) was obtained in other works [53, 54, 55]. If beam splitter is non-symmetric, (4) is generalized to a more complicated form [53, 55]. For a symmetric beam splitter, we can choose $\delta_t = 0$, which leads to $\delta_r = \pi/2$. In this case, we obtain $r_1 = \mathrm{e}^{\mathrm{i}\pi/2}\sqrt{R}_1 = \mathrm{i}\sqrt{R}_1$ and $t_1 = \sqrt{T}_1$. Thus, $\hat{S}_1$ operator can be written as:

$$\hat{\mathbf{S}}_1 = \mathrm{i}\sqrt{R}_1\left(|s_y\rangle\langle s_x| + |s_x\rangle\langle s_y|\right) + \sqrt{T}_1\,\hat{\mathbf{I}}_{\mathrm{T}}. \tag{5}$$

The complex factor i in the first term embeds the condition (4) into the equation (5). For the second beam splitter, we can adopt the same procedure. The operator $\hat{\mathbf{S}}_2$ which represents its action is formally analogous to $\hat{\mathbf{S}}_1$. Thus, this operator is $\hat{\mathbf{S}}_2 = \mathrm{i}\sqrt{R}_2\left(|s_y\rangle\langle s_x| + |s_x\rangle\langle s_y|\right) + \sqrt{T}_2\rangle\,\hat{\mathbf{I}}_{\mathrm{T}}$.

2.2.2. The quantum operator representing the action of mirrors

The action of the ideal and totally reflective mirrors configured in a Mach-Zehnder interferometer is readily seen in Figure 1. It changes the translational state of the photon from $|s_x\rangle$ to $|s_y\rangle$ and vice-versa. Also, it adds a π phase change on the reflected photon. Thus:

$$\hat{\mathbf{M}} = \mathrm{e}^{\mathrm{i}\pi}\left(|s_x\rangle\langle s_y| + |s_y\rangle\langle s_x|\right) = -|s_x\rangle\langle s_y| - |s_y\rangle\langle s_x| \tag{6}$$

Note that the π phase change acts as a global phase (when calculating probabilities, this phase will not contribute). We decided to maintain this global phase

in expression (6) for didactical purposes. It is easy to show that $\hat{\mathbf{M}}\,|s_x\rangle = -|s_y\rangle$ and $\hat{\mathbf{M}}|s_y\rangle = -|s_x\rangle$. This operator is both unitary and hermitian, since $\hat{\mathbf{M}}^\dagger = -|s_y\rangle\langle s_x| - |s_x\rangle\langle s_y| = \hat{\mathbf{M}}$ and $\hat{\mathbf{M}}^\dagger\hat{\mathbf{M}} = \hat{\mathbf{M}}\hat{\mathbf{M}} = \left(-|s_x\rangle\langle s_y| - |s_y\rangle\langle s_x|\,\right)\left(-|s_y\rangle\langle s_x| - |s_x\rangle\langle s_y|\right) = |s_x\rangle\,\langle s_x| + |s_y\rangle\langle s_y| = \hat{\mathbf{I}}_{\mathrm{T}}$ This operator acts once in each arm of the interferometer.

2.2.3. Phase shifts due to path difference in two arms of the interferometer

Considering that two virtual photon sources can be associated to each screen on the exit ports 1 and 2 of MZI (double-slit analogy), for each screen there are two possible paths associated with quantum translational states of the photon, emerging a phase difference φ between them. As defined by Omnès [56, p. 371], φ is the phase difference between two semiclassical paths going through each arm, respectively, and ending at a point (x_i, y_i) of the i-th screen ($i = 1, 2$). It is possible to deduce this phase difference from time evolution operator, but we will not perform this calculation here. Considering that is the phase difference that produces interference (the relative phase), we consider that the arm A introduces a phase φ and the arm B does not introduce any phase. This action can be represented by means of an operator, which we call $\hat{\mathbf{\Phi}}$. Assuming that the action of this operator occurs after the action of the mirrors, as shown in Figure 1, we can infer its mathematical form. After the mirrors, the translational state associated with the arm A of the interferometer is $|s_y\rangle$. So, the operator $\hat{\mathbf{\Phi}}$ must contain two terms: one projects the translational state of the photon onto $|s_x\rangle$ without inserting a phase; the other projects onto $|s_y\rangle$ inserting a phase φ. Thus, this operator can be written as:

$$\hat{\mathbf{\Phi}} = |s_x\rangle\,\langle s_x| + \mathrm{e}^{\mathrm{i}\varphi}|s_y\rangle\langle s_y|. \tag{7}$$

Constructed with requirements above, this operator must act after the operator $\hat{\mathbf{M}}$. This operator is also unitary, since $\hat{\mathbf{\Phi}}^\dagger\hat{\mathbf{\Phi}} = \left(|s_x\rangle\,\langle s_x| + \mathrm{e}^{-\mathrm{i}\varphi}|s_y\rangle\langle s_y|\right)\left(|s_x\rangle\,\langle s_x| + \mathrm{e}^{\mathrm{i}\varphi}|s_y\rangle\langle s_y|\right) = \hat{\mathbf{I}}_{\mathrm{T}}$. We now have all mathematical tools needed to describe the action of the interferometer on initial translational states of the photon.

2.2.4. The action of the Mach-Zehnder interferometer and the quantum interference on both screens

The evolution of initial translational state of the photon (input state) as it propagates inside the interferometer can be described by means of successive actions of the operators defined above. These actions, in each arm, occurs in the following order: action of the first beam splitter, action of the mirror, action due to the phase shift and, finally, action of the second beam splitter. Thus, the global action of the Mach-Zehnder on the input translational state of the photon can be described by an operator $\hat{\mathbf{Z}}$, which is given by the product of the operators defined in previous section and in the order cited above. So, considering an incident photon coming from input port I, $\hat{\mathbf{Z}}{=}\hat{\mathbf{S}}_2\hat{\mathbf{\Phi}}\hat{\mathbf{M}}\hat{\mathbf{S}}_1$ and its action on the initial translational state of the photon will be written as $\hat{\mathbf{Z}}\,|s_x\rangle = \hat{\mathbf{S}}_2\hat{\mathbf{\Phi}}\hat{\mathbf{M}}\hat{\mathbf{S}}_1\,|s_x\rangle$ (this operator is also unitary, since it is obtained from a product of four unitary operators). In each case, the action of these operators occurs in the right-to-left order, obeying the order cited above (beam splitter 1-mirror-phase shift-beam splitter 2). The state at the output ports will be named as $|\Psi_{\mathrm{out}}\rangle = \hat{\mathbf{Z}}\,|s_x\rangle$. The following steps show each change (intermediate states) of the initial translational state of the photon as it interacts with the devices in the interferometer, until the final state $|\Psi_{\mathrm{out}}\rangle$:

$$\begin{aligned}
|\Psi_{\mathrm{in}}\rangle &= |s_x\rangle \xrightarrow{\hat{\mathbf{S}}_1\ \text{(first beam splitter)}} \mathrm{i}\sqrt{R_1}|s_y\rangle \\
&+\sqrt{T_1}\,|s_x\rangle \xrightarrow{\hat{\mathbf{M}}\ \text{(mirror)}} -\mathrm{i}\sqrt{R_1}\,|s_x\rangle - \sqrt{T_1}|s_y\rangle \\
&\xrightarrow{\hat{\mathbf{\Phi}}\ \text{(phase shift)}} -\mathrm{i}\sqrt{R_1}\,|s_x\rangle - \mathrm{e}^{\mathrm{i}\varphi}\sqrt{T_1}|s_y\rangle \\
&\xrightarrow{\hat{\mathbf{S}}_2\ \text{(second beam splitter)}} -\mathrm{i}\sqrt{R_1}\left(\sqrt{T_2}\,|s_x\rangle\right. \\
&\left.+\mathrm{i}\sqrt{R_2}|s_y\rangle\right) - \mathrm{e}^{\mathrm{i}\varphi}\sqrt{T_1}\left(\mathrm{i}\sqrt{R_2}\,|s_x\rangle + \sqrt{T_2}|s_y\rangle\right) \\
&= |\Psi_{\mathrm{out}}\rangle\,.
\end{aligned} \tag{8}$$

Finally, rearranging terms in the last expression of the above chain, it can be shown that the output state is:

$$\begin{aligned}
|\Psi_{\mathrm{out}}\rangle = \hat{\mathbf{Z}}\,|s_x\rangle = &-\mathrm{i}\left[\sqrt{R_1T_2} + \mathrm{e}^{\mathrm{i}\varphi}\sqrt{R_2T_1}\right]|s_x\rangle \\
&+\left[\sqrt{R_1R_2} - \mathrm{e}^{\mathrm{i}\varphi}\sqrt{T_1T_2}\right]|s_y\rangle.
\end{aligned} \tag{9}$$

The factor multiplying $|s_x\rangle$ in (9) is the probability amplitude that a photon exits through output port 1 and hits the corresponding screen. The squared modulus of $\sqrt{R_1T_2}$ equals to R_1T_2 and is interpreted as the joint probability of photon reflection by the first beam splitter *and* transmission by the second, being associated to path B and exiting by the port 1. The square modulus of the second term equals to R_2T_1 and is interpreted as joint probability of photon transmission by the first beam splitter *and* reflection by the second, being associated to path A and equally exiting by port 1. Similar reasoning can be used to interpret the term multiplying $|s_y\rangle$. The squared modulus of first term is the joint probability of photon reflection by both beam splitters, being associated to path B and exiting by output port 2. The squared modulus of the second term is the joint probability of photon transmission by both beam splitters, being associated to path A and exiting by the port 2. These squared moduli yield the probability distributions on each screen, as explained in the next section.

2.2.5. Probability distribution on the screens: quantum interference patterns

Probability distributions on each screen can be easily obtained from probability amplitudes in (9). We

 DOI: http://dx.doi.org/10.1590/1806-9126-RBEF-2019-0283

must perform a simple calculation for each screen: $P_1(\varphi) = |\langle s_x \mid \Psi_{\text{out}}\rangle|^2 = \langle \Psi_{\text{out}} \mid s_x\rangle \langle s_x \mid \Psi_{\text{out}}\rangle$ and $P_2(\varphi) = |\langle s_y|\Psi_{\text{out}}\rangle|^2 = \langle \Psi_{\text{out}}|s_y\rangle\langle s_y|\Psi_{\text{out}}\rangle$. Nonetheless, it is adequate to interpret these expressions in a physical framework, instead of appealing to a pure mathematical procedure. In quantum picture of MZI, we consider that the photon hits a particular point of the screen and produces a punctual mark on it. An interference pattern is gradually being formed until it becomes clearly discernible (right side of Figure 1). It is known that the detection probability of a photon in a given point of a particular screen is proportional to the intensity at this point. In other words, $P_1(\varphi) \propto I_1(\varphi)$ and $P_2(\varphi) \propto I_2(\varphi)$ [57, p. 788]. Thus, the distribution of punctual marks in each screen has similar mathematical form as classical intensities, i.e., photon marks will appear most in regions of greater intensity and less on regions of lower intensity.

We consider that each screen is subdivided in several very small square regions. When a photon hits this small region, it produces a punctual red mark, reinforced if subsequent photons hit this same region. Thus, we conceive each of these very small regions as a small detector. The probability distribution on the screens can be obtained calculating the probability that a photon hits a particular small detector. Quantum physics provide a way to perform this calculation: each small detector on screen 1 measures the observable $\hat{\mathbf{\Pi}}_x = |s_x\rangle\langle s_x|$. This observable has two eigenvalues: 0 (no detection and no punctual mark produced) and 1 (detection of a photon and a punctual red mark produced). Thus, the probability distribution on screen 1 is given by the expected value of the observable $\hat{\mathbf{\Pi}}_x$ in the state $|\Psi_{\text{out}}\rangle$:

$$\begin{aligned} P_1(\varphi) &= \langle \Psi_{\text{out}}| \hat{\mathbf{\Pi}}_x |\Psi_{\text{out}}\rangle = R_1T_2 \\ &+ R_2T_1 + 2\sqrt{R_1R_2T_1T_2}\cos\varphi. \end{aligned} \quad (10)$$

The same reasoning holds for screen 2. In this case, the probability distribution is given by:

$$\begin{aligned} P_2(\varphi) &= \langle \Psi_{\text{out}}| \hat{\mathbf{\Pi}}_y |\Psi_{\text{out}}\rangle = R_1R_2 + T_1T_2 \\ &- 2\sqrt{R_1R_2T_1T_2}\cos\varphi. \end{aligned} \quad (11)$$

where $\hat{\mathbf{\Pi}}_y = |s_y\rangle\langle s_y|$. Note that expressions (10) and (11) are formally identical to that obtained by means of the classical picture (considering that source emits an electromagnetic wave – a laser beam), depicted in expressions (4) and (5) in Cavalcanti, *et al.* [1, p. 8].

Since φ depends on position x of screen, because $\varphi(x) = [2\pi\delta/(\lambda\Delta)]\,x$, where $\Delta = (s+L)\cos 2\alpha + L + l$ [see reference 1, Figure 2], the probabilities also depend on x. Rigorously speaking, probabilities given by (10) and (11) are the probabilities that a photon hits some specific point x on screen (a very small detector, as said right above), being larger near regions where constructive interference occurs (maxima) and lesser near regions where destructive interference occurs (minima). In practice these probabilities also depend on y, since diffraction also occurs (see Figure 2).

However, diffraction acts in order to concentrate photon incidence around the central region of the screens, since Airy function modulates overall probabilities so that they are much larger in these regions than on the borders[6] (as we can see from the interference patterns shown in figures 1 and 2).

The visibility in each screen is obtained from expressions (10) and (11). For screen 1, we obtain

$$\begin{aligned} \mathcal{V}_1 &= \frac{P_{1\max} - P_{1\min}}{P_{1\max} + P_{1\min}} = \frac{P_1(\varphi=0) - P_1(\varphi=\pi)}{P_1(\varphi=0) + P_1(\varphi=\pi)} \\ &= \frac{2\sqrt{R_1R_2T_1T_2}}{R_1T_2 + R_2T_1}, \end{aligned} \quad (12)$$

and, for screen 2,

$$\begin{aligned} \mathcal{V}_2 &= \frac{P_{2\max} - P_{2\min}}{P_{2\max} + P_{2\min}} = \frac{P_2(\varphi=\pi) - P_2(\varphi=0)}{P_2(\varphi=\pi) + P_2(\varphi=0)} \\ &= \frac{2\sqrt{R_1R_2T_1T_2}}{R_1R_2 + T_1T_2}. \end{aligned} \quad (13)$$

Figure 2 shows two examples of classical and quantum patterns (profiles and resulting patterns on screen 1). These visibilities are important to stablish a *quantitative complementarity principle*, developed in the following sections.

2.3. Wave-particle complementarity on the MZI

2.3.1. A quantitative approach to complementarity in the context of MZI

Complementarity is a central concept of the *Copenhagen Interpretation* and it is a complex principle of Quantum Physics [40, p. 85-107, 58, p. 135-150]. For the sake of simplicity, we restrict our approach in one of the forms by which complementarity is known (the one that is more popular in university textbooks): the complementarity between wave and particle behavior of quantum objects. In the MZI (Figure 1) and other two-way interferometers, this form of complementarity may be stated as follows [59, p. 43]: if in the interferometer we don't know anything about which path (A or B) the photon (quantum object) is associated with, interference pattern arises on each of the screens with maximum contrast (visibility equal to 1). On the other hand, if the path associated

[6] It is possible that a photon does not hit a screen after exiting the output ports 1 or 2, propagating out of its limits. This can happen because Airy function is very small (but not rigorously null) at points away from the center of screens. However, in real situations interference patterns can have diameter of millimeters, causing all photons to hit the recording device. Interference patterns are clearly visible only when amplified by auxiliary devices – single photon interference patterns are not usually registered directly on screens like that shown in our software. These experiments sometimes are carried using image intensified CCD cameras and the "image" of interference can be seen and processed on a computer screen. In our software, for didactical purposes (and so, avoiding unnecessary complications), we consider that this "image" forms directly on the screens and that they are large enough so that every single photon emitted by the source hits them.

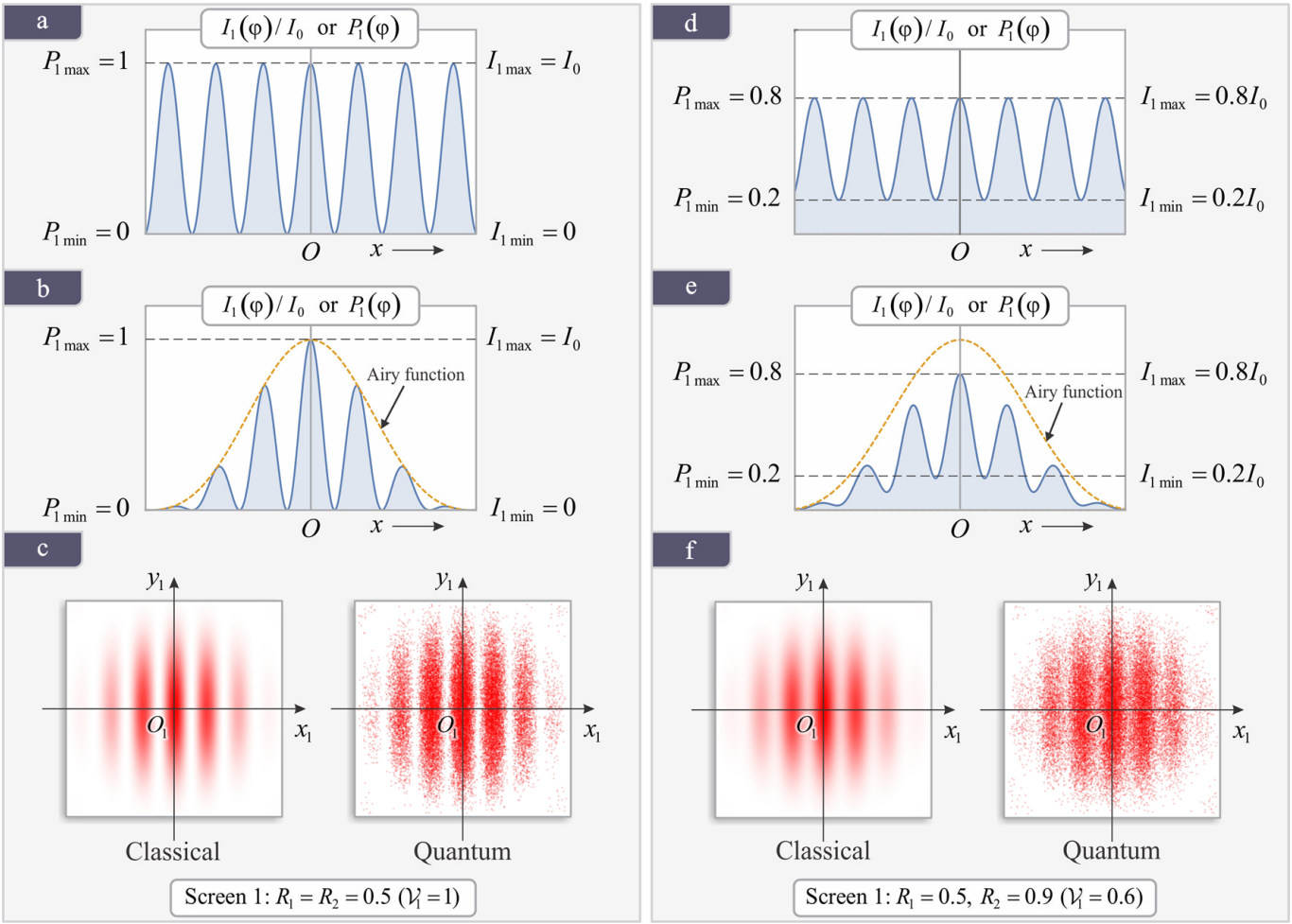

Figure 2: (a) Plotted intensity (classical) or probability (quantum – see section 2.2) profile on screen 1, neglecting diffraction effects, for $R_1 = R_2 = 0.5$ (balanced beam splitters). In this situation, $I_{1\max} = I_0$ ($P_{1\max} = 1$) and $I_{1\min}$ ($P_{1\min} = 0$), leading to maximum visibility ($\mathcal{V}_1 = 1$). (b) The same profile as (a) but considering diffraction (Airy function modulates the intensity). (c) Resulting classical and quantum patterns on screen 1 for $R_1 = R_2 = 0.5$. (d) Same as (a), but now considering $R_1 = 0.5$ and $R_2 = 0.9$. In this case we obtain $I_{1\max} = 0.8I_0$ ($P_{1\max} = 0.8$) and $I_{1\min} = 0.2I_0$ ($P_{1\min} = 0.2$), leading to $\mathcal{V}_1 = 0.6$. (e) Same profile as (d) but considering diffraction. (f) Resulting classical and quantum patterns on screen 1 for $R_1 = 0.5$ and $R_2 = 0.9$. Patterns on the left (c), with maximum contrast, are sharper than patterns on right (f), in which contrast is 0.6 (despite the lower contrast, the interference effect is clearly discernible).

with each photon hitting the screens is completely distinguishable, no interference will arise on them (visibility equal to 0). Therefore, path distinguishability, or ability to take a "trajectory" inside the interferometer (a particle-like behavior), and ability to produce interference pattern (wave-like behavior) are *complementary* or mutually exclusive behaviors. There is no way to configure the interferometer so that the photons could exhibit these two behaviors at once in the same experiment and on the same screen.

As first shown by Wootters and Zurek [60], by means of a *gedankenexperiment*, these two situations are particular extreme cases – it is possible to obtain intermediate situations in which there are some available information about the path associated with the quantum object (encoded in its quantum state) together with discernible interference patterns on the screens (with visibility less than one). Almost ten years later, Greenberger and Yasin [61] have developed and conducted an experiment reinforcing this prediction. To better understand this intermediate behavior, we must quantitatively define the *path distinguishability* in the interferometer, emphasizing how it relates to the visibility of the interference pattern, leading to a quantitative form of complementarity principle between wave-like and particle-like behavior. This relation was contained implicitly in the work of Wootters and Zurek [60] and was obtained independently by Jaeger, *et al.* [62] and Englert [63], being expressed in the following form:

$$\mathcal{D}^2 + \mathcal{V}^2 \leq 1, \tag{14}$$

where D and V are, respectively, the path distinguishability and visibility of the interference pattern (both can take values between 0 and 1, satisfying the above inequality). In the case that the quantum objects are prepared

 DOI: http://dx.doi.org/10.1590/1806-9126-RBEF-2019-0283

in a quantum pure state, the inequality (14) reduces to the following equality[7]:

$$\mathcal{D}^2 + \mathcal{V}^2 = 1. \tag{15}$$

Recently, an equivalent quantitative form of wave-particle complementarity has been proposed, relying on complementarity between quantum coherence and path distinguishability [64, 65]. Here, we will use the more common form defined in (14) or (15). These relations have been experimentally tested in different contexts along past years [41, 42, 66], including in the MZI with an unbalanced beam splitter [67][8] and with an unbalanced beam splitter in a delayed-choice regime [68].

In Mach-Zehnder interferometer, distinguishability may be interpreted as the knowledge degree about the path associated with the photon in the interferometer. In other words, it is a physical parameter that can be used to quantify the particle-like character of the photon [60, 61]. The visibility may be interpreted as a physical parameter that quantifies its wave-like character [60, 61]. Since all the incident photons are prepared in a pure state after its interaction with the first beam splitter (see footnote 7), equation (15) holds and it clearly points that the more (less) particle-like the quantum object behaves inside the interferometer, less (more) evident is the wave-like behavior on the screens. It is important to emphasize that, although simultaneous partial knowledge about the path associated with the photon and clear interference patterns on the screens are possible to be obtained in the same experiment, it does not violate the complementarity principle. The duality relations (14) or (15) shows that the degree of one behavior (wave-like or particle-like) increases at the expense of decreasing the other respecting the limits imposed by (14) or (15), extending complementarity between these behaviors to situations beyond the extreme cases discussed by Bohr[9]. According to Wootters and Zurek [60], equations (14) and (15) point the possibility that photons exhibit simultaneously partial particle-like and wave-like behaviors.

[7] When the MZI is configured similar to what is shown in Figure 1, with two beam splitters, all photons are prepared in a superposition of translational states after interaction with the first unbalanced beam splitter [13], except for the extreme values $R_1 = 0$ ($T_1 = 1$) or $R_1 = 1$ ($T_1 = 0$). So, each incident photon is prepared in a pure state, like that given in (2) or (3). For didactical purposes, we simplify our approach and will not consider situations that involve mixed states here (which would require use of *density operator* formalism). For the reader interested in deepening their knowledge about mixed states, we recommend the works of Jaeger*, et al.* [62] and Auletta*, et al.* [39] for additional details concerning mixed states.

[8] The authors of this paper use the term *asymmetric beam splitter* to describe what we define as *unbalanced beam splitter*. In our work the term *asymmetric* was employed to define beam splitters which show different responses to the beam, depending on the input port in which the incidence occurs.

[9] Bohr had considered extreme situations in which complete path information is available in conjunction with total lack of interference, corresponding to a full particle-like behavior ($\mathcal{D} = 1$ and $\mathcal{V} = 0$) or the complementary one, in which none knowledge about path is available and interference arises with maximum visibility, corresponding to full wave-like behavior ($\mathcal{V} = 1$ and $\mathcal{D} = 0$).

In the following sections, we will obtain explicit formulas for the distinguishability $\mathcal{D}$ in the context of MZI, in a different and more intuitive way than that adopted by Jaeger*, et al.* [62], Englert [63] and others. In their works, advanced mathematical formalism has been employed to obtain relations in the context of general two-way interferometers. For didactical reasons, we choose to avoid the use of this formalism here. In next sections, two classes of distinguishability will be discussed.

2.3.2. Predictability or a priori path distinguishability

The *a priori* distinguishability [63, 68], as known as *predictability*, is defined in terms on the reflection and transmission probabilities of the first beam splitter. If it is unbalanced, this, by itself, provides information about the path associated with each incident photon, even before its interaction with the first beam-splitter (this is why we call this as *predictability* or *a priori* distinguishability). To deduce a quantitative form of predictability, one must to find a betting strategy that maximizes the probability of guessing right the path associated with the photon after its interaction with first beam splitter. As stated in section 2.2, the first unbalanced beam splitter produces two possible outcomes after interaction with each photon: it transforms the translational state of the photon in a linear superposition of $|s_x\rangle$ (associated with transmission and path A) and $|s_y\rangle$ (associated with reflection and path B), with unbalanced probabilities T_1 and R_1, respectively.

The ability to assign a path to the photon is closely related to predictability, which in turn is closely related to the probability of making successful guess about the path associated with the photon after its interaction with first beam splitter, as we will show now. Having prior knowledge about the reflection probability R_1 (and consequently the transmission probability $T_1 = 1 - R_1$), the betting strategy to maximize the probability of guessing right the path is choose the one that contribute most [42, 66]. If a detector were placed in arm A, it would trigger N_A times, where $N_\mathrm{A} \approx T_1 N_\mathrm{F}$ (see Figure 1) – recalling that N_F is the total number of photons emitted by the source. This is the estimated number of photons associated with path A. The remaining photons $N_\mathrm{B} = N_\mathrm{F} - N_\mathrm{A} \approx R_1 N_\mathrm{F}$ would not trigger the detector, being associated with path B. These are the only two possible outcomes after the interaction with the first beam splitter. In the case when $R_1 \neq T_1$, in order to maximize the probability of making a correct guess about the path associated with each photon, the obvious choice is to bet in the path with greater probability of occurrence: if $T_1 > R_1$ ($R_1 < T_1$) the choice that maximizes this probability is path A (B). Summarizing, the probability of making a successful guess about the path associated with the photon after its interaction with first beam splitter

is:

$$P_{\text{ms}} = \text{Max}\{R_1, T_1\} = \frac{1}{2}(R_1 + T_1) + \frac{1}{2}|R_1 - T_1| = \frac{1}{2} + \frac{1}{2}|R_1 - T_1|. \quad (16)$$

In the above expression, we used the identity $\text{Max}\{x,y\} = (x+y)/2 + |x-y|/2$. Furthermore, the subscript *ms* means maximum (m) and success (s) of correctly guessing the path. When $R_1 = T_1 = 1/2$ only the first term (1/2) remains. This is the probability when no *a priori* path information is available and the result of interaction of the photon with first beam splitter is completely unpredictable, as are the outcomes of a regular coin toss – heads or tails game (considering an unbiased coin). Therefore, both reflection (path B) and transmission (path A) of a photon occurs randomly in equal proportions, turning impossible statistically distinguish these two outcomes (and so the paths A and B). When $R_1 \neq T_1$ the second term of (16) leads P_{ms} to be greater than 1/2 and the term $\mathcal{P} = |R_1 - T_1| = |2R_1 - 1|$ can be interpreted as *a priori path distinguishability* or *predictability*, which assumes values between 0 and 1. Thus, (16) can be written as

$$\mathcal{P}_{\text{ms}} = \frac{1 + P}{2}. \quad (17)$$

When $R_1 = 0$ (equivalent to remove first beam splitter) the path associated with the photon can only be A and $\mathcal{P} = 1$, corresponding to full path predictability. When $R_1 = 1$ (equivalent to put an ideal mirror in place of first beam splitter) the path associated can only be B, leading also to $\mathcal{P} = 1$. In both these cases the initial translational state of the photon is not transformed into a linear superposition of translational states: when $R_1 = 0$ the translational state remains $|s_x\rangle$ (path A) and when $R_1 = 1$ it is transformed to $|s_y\rangle$ (path B), resulting in full particle-like behavior. This condition is sufficient to vanish the interference patterns on the screens, as it will be shown in the following section. Intermediate values such that $0 < \mathcal{P} < 1$ lead to interference patterns with visibility less than 1. Note that even when no measurement is performed in the interferometer's arms, the pattern visibility will decrease due only to the availability of *a priori* path information. This can be deduced by (12) and (13), substituting $4R_1T_1 = 1 - \mathcal{P}^2$ in both expressions, leading to

$$\mathcal{V}_1 = \frac{\sqrt{(1 - \mathcal{P}^2) R_2T_2}}{R_1T_2 + R_2T_1}, \quad (18)$$

and

$$\mathcal{V}_2 = \frac{\sqrt{(1 - \mathcal{P}^2) R_2T_2}}{R_1R_2 + T_1T_2}. \quad (19)$$

2.3.3. A posteriori distinguishabilities

This class of path distinguishability is related to availability of path information *after* the photon interacts with first beam splitter. It can also be retrieved inserting non-demolition detectors (which-way detectors) or polarization filters in the arms of the interferometer. However, in this paper these situations will not be addressed, in order to avoid detailing more advanced concepts that require explicit use of more sophisticated mathematical formalism (composite states, entanglement, density operator and others). The unbalance of beam splitters itself is sufficient to provide path information [66, 68] and only this possibility will be considered here. In the literature there are some interesting works addressing the concept of path information acquired by which-way detectors and/or polarization filters [10, 13, 69], topic that also has been addressed in didactical context [70].

If the reflection and transmission probabilities of both beam splitters are known, it is possible to adopt the same betting strategy to guess the path associated with the photons discussed in previous sections. In Figure 1, the estimated number of photons that hit each screen is shown. If the source emits N_{F} photons, the approximate number of photons N_1 and N_2 which respectively hit screens 1 and 2 can be obtained from (10) and (11), by taking the mean in one complete oscillation of $\cos\varphi$, i.e.:

$$N_1 \approx \frac{1}{2\pi}\int_0^{2\pi} P_1(\varphi)\, N_{\text{F}} d\varphi = (R_1T_2 + R_2T_1)\, N_{\text{F}} = P_{\text{S1}} N_{\text{F}}, \quad (20)$$

and

$$N_2 \approx \frac{1}{2\pi}\int_0^{2\pi} P_2(\varphi)\, N_{\text{F}} d\varphi = (R_1R_2 + T_1T_2)\, N_{\text{F}} = P_{\text{S2}} N_{\text{F}}. \quad (21)$$

The meaning of terms on the right-hand side (20) or (21) is clear. Considering (20), the quantity R_1T_2 is the probability of a photon to be reflected by first beam splitter *and* transmitted by the second, exiting from output port 1. In this case, the photon is associated with path B and we define $N_{1\text{B}} \approx R_1T_2N_{\text{F}}$ as the approximate number of photons that hit the screen 1 and can be associated with the path B. The second term, R_2T_1, is the probability that a photon is transmitted by the first beam splitter *and* reflected by the second, also exiting from output 1. So, the photon is associated with path A in this case and we define $N_{1\text{A}} \approx R_2T_1N_{\text{F}}$ as the approximate number of photons that hit the screen 1 and can be associated with the path A. The total number of photons exiting from output port is approximately $N_1 = N_{1\text{A}} + N_{1\text{B}} \approx (R_1T_2 + R_2T_1)\, N_{\text{F}}$. The same reasoning can be used to the output port 2 (screen 2), described by (21): we can define $N_{2\text{B}} \approx R_1R_2N_{\text{F}}$ ($N_{2\text{A}} \approx T_1T_2N_{\text{F}}$) as the approximate number of photons that hit screen 2 and can be associated with path B (A), so that $N_2 = N_{2\text{A}} + N_{2\text{B}} \approx (R_1R_2 + T_1T_2)\, N_{\text{F}}$. Analogously, $P_{\text{S2}} = R_1R_2 + T_1T_2$ is the mean probability of photon incidence on screen 2. So, expressions (10) and (11) can be rewritten into

$$P_1(\varphi) = P_{\text{S1}}(1 + \mathcal{V}_1 \cos\varphi), \quad (22)$$

and

$$P_2(\varphi) = P_{S2}(1 - \mathcal{V}_2 \cos\varphi). \quad (23)$$

Considering the screen 1, we define p_{1A} as the probability that some punctual mark on this screen has been produced by a photon that is associated to path A. It is given by the ratio between the approximate number of photons exiting by output port 1 associated to path A ($N_{1A} \approx R_2T_1N_F$) and the total number of photons exiting by this output port ($N_1 = N_{1A}+N_{1B} \approx (R_1T_2 + R_2T_1)N_F$). Namely,

$$p_{1A} = \frac{N_{1A}}{N_1} = \frac{R_2T_1}{R_1T_2 + R_2T_1} \quad (24)$$

The same reasoning leads to obtention of p_{1B}, the probability that some punctual mark on this screen has been produced by a photon that is associated to path B:

$$p_{1B} = \frac{N_{1B}}{N_1} = \frac{R_1T_2}{R_1T_2 + R_2T_1}. \quad (25)$$

It is evident that $p_{1A} + p_{1B} = 1$.

Now the betting strategy consists in choosing a particular punctual mark in this screen and make a guess about which path is associated with the photon which produced it (there are two possible outcomes, A or B). This involves again a betting strategy of making guesses about two possible outcomes with unequal probabilities, in this case p_{1A} and p_{1B}. As discussed in previous sections, now the maximum probability of guessing right the path associated with a photon that exits the interferometer and hits screen 1 is

$$P_{1ms} = \text{Max}\{p_{1A}, p_{1B}\} = \frac{1}{2}(p_{1A} + p_{1B}) + \frac{1}{2}|p_{1A} - p_{1B}| = \frac{1}{2} + \frac{1}{2}\frac{|R_1T_2 - R_2T_1.|}{R_1T_2 + R_2T_1}. \quad (26)$$

Thus, the term $|R_2T_1 - R_1T_2|/(R_1T_2 + R_2T_1)$ is defined as *a posteriori path distinguishability* concerning photons that hit screen 1 (henceforward we will simply call *distinguishability*). For photons that hit the screen 2 we have

$$p_{2A} = \frac{N_{2A}}{N_2} = \frac{T_1T_2}{R_1R_2 + T_1T_2} \quad (27)$$

and

$$p_{2B} = \frac{N_{2B}}{N_2} = \frac{R_1R_2}{R_1R_2 + T_1T_2} \quad (28)$$

and so, the same reasoning developed on screen 1 can be used. Thus, the distinguishabilities for screens 1 and 2 are, respectively

$$\mathcal{D}_1 = \frac{|R_1T_2 - R_2T_1|}{R_1T_2 + R_2T_1} = \sqrt{1 - \frac{4R_1R_2T_1T_2}{(R_1T_2 + R_2T_1)^2}} = \sqrt{1 - (1 - \mathcal{P}^2)\frac{R_2T_2}{(R_1T_2 + R_2T_1)^2}} = \sqrt{1 - 4p_{1A}p_{1B}}, \quad (29)$$

and

$$\mathcal{D}_2 = \frac{|R_1R_2 - T_1T_2|}{R_1R_2 + T_1T_2} = \sqrt{1 - \frac{4R_1R_2T_1T_2}{(R_1R_2 + T_1T_2)^2}} = \sqrt{1 - (1 - \mathcal{P}^2)\frac{R_2T_2}{(R_1R_2 + T_1T_2)^2}} = \sqrt{1 - 4p_{2A}p_{2B}}. \quad (30)$$

To obtain the second equality we used the identity $\mathcal{P}^2 = 1 - 4R_1T_1$. Using (12) and (13) in (29) and (30), respectively, it is easy to verify the equalities $\mathcal{D}_1^2 + \mathcal{V}_1^2 = 1$ and $\mathcal{D}_2^2 + \mathcal{V}_2^2 = 1$. Also, we have $P_{1ms} = (1 + \mathcal{D}_1)/2$ and $P_{2ms} = (1 + D_2)/2$. Furthermore, it is straightforward to show that $\mathcal{D}_1 = \mathcal{D}_2 = \mathcal{P}$ when the second beam splitter is balanced, i.e., path information comes exclusively from predictability in this situation. The visibilities also can be written in terms of probabilities p_{iA} and p_{iB} for each screen. It is straightforward to show that $\mathcal{V}_1 = 2\sqrt{p_{1A}p_{1B}}$ and $\mathcal{V}_2 = 2\sqrt{p_{2A}p_{2B}}$.

Extreme complementary situations occur on both screens when (i) two beam splitters are balanced, leading to $\mathcal{D}_1 = \mathcal{D}_2 = 0$, causing interference patterns to arise on both screens with maximum contrast, i.e., $\mathcal{V}_1 = \mathcal{V}_2 = 1$, and when (ii) $R_1R_2T_1T_2 = R_1R_2(1 - R_1)(1 - R_2) = 0$, leading to full path distinguishability on both screens ($\mathcal{D}_1 = \mathcal{D}_2 = 1$) and no interference at all ($\mathcal{V}_1 = \mathcal{V}_2 = 0$), except when the pair (R_1R_2) equals to $(0, 0)$, $(1, 0)$, $(0, 1)$ or $(1, 1)$ – in this case, photons hit only one of the screens [in reference 1, see Figure 4 and the subsequent discussion], where no interference occurs (visibility 0, distinguishability 1). This last situation includes cases in which $\mathcal{P} = 1$. Most physics textbooks refer only to these complementary situations, in which interference occurs with maximum contrast if no path information is available or in which interference vanishes completely when we are sure about the path associated with the quantum object [57, 71, 72, 73, 74].

In intermediate situations, the larger the visibility (degree of wave-like behavior) the lower the distinguishability (degree of particle-like behavior) and vice-versa. Both predictability and distinguishability relate to the available amount of path information [61]. If some amount of path information is available, the contrast of interference pattern will be reduced according to relation (14) or (15).

Note that this phenomenon occurs even if no measurement is performed to find the photon in the arm A or B: the availability of path information is sufficient to decrease the visibility of interference pattern. This description goes far beyond extreme situations and points the importance of complementarity principle in order to understand complementarity between situations in which there is coexisting wave-like and particle-like behaviors of the photon in MZI. Consider the situation shown in Figure 2 (quantum pattern), where $R_1 = 0.5$ (first beam splitter is balanced), $R_2 = R$ and $T_2 = 1-R$, with $R \neq T$ (second beam splitter is unbalanced). In this case, the visibilities and distinguishabilities are identical on each screen, given by $\mathcal{V}_1 = \mathcal{V}_2 = \mathcal{V} = \sqrt{2RT} = \sqrt{2R(1 - R)}$ and $\mathcal{D}_1 = \mathcal{D}_2 = \mathcal{D} = |1 - 2R|$, respectively. The probability of making a correct guess about the path associated with any mark produced on each screen is given by $P_{ms} = (1 + D)/2$. It is worth to point that the probability P_{ms} of guessing right the path associated with the photon is *quantitatively* the same in each screen, but not *qualitatively* the same. It is easy to show in this case that $p_{1A} = p_{2B} = R$ and $p_{1B} = p_{2A} = T = 1 - R$.

When $R > 0.5$ we have $p_{1A} = R > p_{1B} = 1 - R$ and the path that represents the best choice to maximize P_{ms} on screen 1 is the path A. On screen 2, we have $p_{2A} = 1 - R < p_{2B} = R$ and the best choice is the path B. When $R < 0.5$, the opposite occurs: the best choice to maximize P_{ms} on screens 1 and 2 is the path B and A, respectively. Figure 3 was designed with both sides showing different colors to stress these qualitative differences between the interference phenomena which arises on each screen.

Moreover, points labelled as a, b and c illustrate a very interesting situation in which a strong coexistence between wave-like and particle-like behavior takes place. For $R = 0.9$ the distinguishability reaches the value 0.8 (point b), leading to an interference pattern with visibility 0.6 (point c). In this case it is possible to correctly guess the path associated with approximately 90 percent (point a) of all photons that hit screen 1 (associated to path A) or 2 (associated to path B) and yet observe an easily discernible interference pattern (although little blurred in comparison with the one with maximum contrast, as shown in Figure 3). A "symmetric" situation happens when $R = 0.1$ (points c, d and e). In this case the same strong coexistence occurs, except that on screen 1 those approximately 90 percent of the photons are now associated to path B, while in screen 2 they are

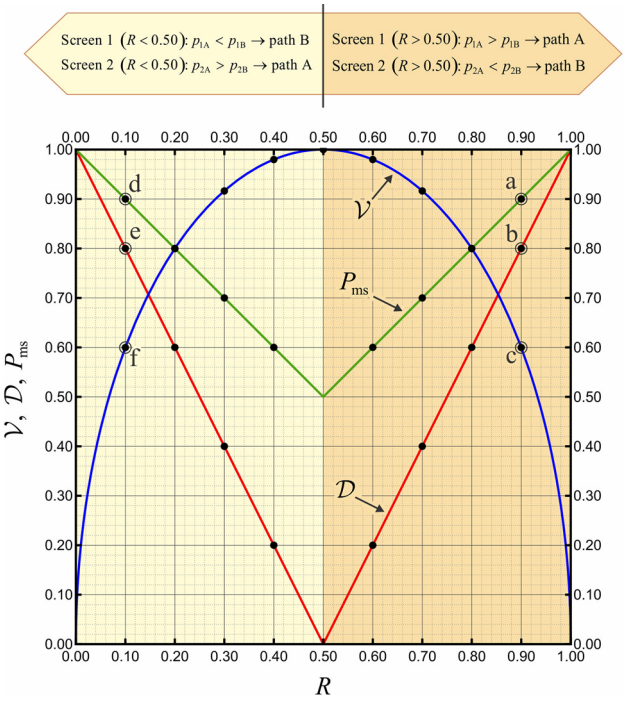

Figure 3: Plot of $\mathcal{V}$, $\mathcal{D}$ and P_{ms} as a function of R (reflection coefficient of the second beam splitter) when the first beam splitter is balanced ($R_1 = T_1 = 0.5$). The second beam splitter is unbalanced with $R_2 = R$ and $T_2 = T$. For these parameters $\mathcal{V}$, $\mathcal{D}$ and P_{ms} are numerically the same on both screens. Left ($R < 0.5$) and right ($R > 0.5$) sides of the graph have different colors and some points are marked to illustrate the discussion which follows in the text.

associated to path A (this is why we used the word *symmetric* between quotation marks).

2.3.4. A posteriori distinguishabilities in a more general framework: quantum state discrimination

Equations (29) and (30) can be obtained by means of a more general framework, considering it as a quantum state discrimination problem on each screen. Consider that the quantum system is prepared in two pure quantum states $|\psi_1\rangle$, with probability p_1, and $|\psi_2\rangle$, with probability p_2. It can be shown that the probability of correctly discriminate these two states with minimum error is given by

$$P_{ms} = \frac{1}{2} + \frac{1}{2}\sqrt{1 - 4p_1p_2\,|\langle\psi_1 \mid \psi_2\rangle|^2}. \qquad (31)$$

This formula was first obtained by Helstrom [75, p. 113] and so it is called *Helstrom Formula*. Its demonstration is beyond the scope of this paper. We invite the interested reader to read the work of Bergou, *et al.* [76, p. 440-443], which provides a demonstration of (31) using the density operator formalism. Since $P_{ms} = (1 + \mathcal{D})/2$, the distinguishability between the states $|\psi_1\rangle$ and $|\psi_2\rangle$ is given by

$$\mathcal{D} = \sqrt{1 - 4p_1p_2\,|\langle\psi_1 \mid \psi_2\rangle|^2}. \qquad (32)$$

It is clear from (32) that $|\psi_1\rangle$ and $|\psi_2\rangle$ are fully distinguishable ($\mathcal{D} = 1$) only when they are orthogonal. Let us move to the context of MZI and consider screen 1 and screen 2 separately. As discussed previously, to hit screen1 a photon may be reflected by the first beam splitter and transmitted by the second (associated to path B, probability R_1T_2) or transmitted by the first beam splitter and reflected by the second (associated to path A, probability R_2T_1). Thus, the probability of a photon be detected on screen 1 is $R_1T_2 + R_2T_1$.

To obtain the distinguishability for screen 1 we can treat this process as a problem of discrimination between the translational states $|\psi_{1A}\rangle = p_{1A}\,|s_x\rangle$ and $|\psi_{1B}\rangle = p_{1B}\,|s_x\rangle$, the translational states of the photons that hit this screen and are associated to path A and B, respectively. We recall that $p_{1A} = R_2T_1/(R_1T_2 + R_2T_1)$ and $p_{1B} = R_1T_2/(R_1T_2 + R_2T_1)$, as defined in (24) and (25). Inserting $|\psi_{1A}\rangle$ and $|\psi_{1B}\rangle$ in (32), we obtain

$$\begin{aligned}\mathcal{D}_1 &= \sqrt{1 - 4p_{1A}p_{1B}\,|\langle s_x \mid s_x\rangle|^2} \\ &= \sqrt{1 - 4p_{1A}p_{1B}}. \end{aligned} \qquad (33)$$

This is exactly what we have in equation (29). Adopting the same reasoning for screen 2, we can easily obtain (30). Distinguishing the path associated to photons that hit a given screen is ultimately to distinguish their two possible translational states, each one associated with one arm of the interferometer.

 DOI: http://dx.doi.org/10.1590/1806-9126-RBEF-2019-0283

2.3.5. Quantifying path information

Until now we have referred to *path information* without propose a more precise definition for it. The focus is the term *information*, which is not trivial to precisely define and quantify [77]. Shannon [78] proposed a way to quantify the lack of information by exploring the link between entropy and the degree of randomness of a system. Despite we are dealing with quantum phenomena, we will discuss the concept of *classical* information that is contained in the outcomes produced by the *classically* read marks that photons produce when hitting a screen. We do not develop here a discussion of information in the framework of quantum physics, which is beyond the scope of this paper.

Entropy is a complex concept which was historically developed from different ways [79]. It is known, from Classical Statistical Physics, that the macroscopic state of a system is characterized by a distribution on its distinct possible microstates. Given a set of possible discrete microstates μ_i, each one with a corresponding probability of occurrence p_i, it can be shown that the entropy of the system depends only on probability distribution of these microstates, namely [80, p. 51, 81, p. 65],

$$S = -k_B \sum_{i=1}^{n} p_i \ln p_i, \tag{34}$$

where k_B is the Boltzmann constant and $\sum_i p_i = 1$. This expression is called *Gibbs Entropy*, despite the fact that Gibbs never wrote this expression with Boltzmann constant. Instead, he claimed that this functional form had properties that can be associated with entropy [81, p. 65]. These remarkable properties of equation (34) are discussed in Pathria and Beale [80, p. 52]. If the system is sure to be found in a ground state ($T = 0$ K) in which we assume that there is one unique possible microstate, we have $p_k = 1$ and all others $p_{i\neq k} = 0$ and the entropy results precisely zero (it is easy to show that $p_i \ln p_i = 0$). In this case, we have full predictability about the system. On the contrary, if the number of accessible states increases, entropy also increases. If all probabilities are equal, such that $p_i = p = 1/n$, the entropy reaches its maximum [81, section 8.2, 82, chapter 11], corresponding to a complete lack of knowledge about the system, of full unpredictability. In this sense, classical entropy can quantify the degree of randomness of a classical system [38, p. 274].

It is possible to define an entropy-like function to quantify partial path information, adopting a slight modified version of the Shannon's mathematical measure of lack of information (which *uses* base-2 logarithm). This was proposed by Zeilinger [83], considering a random variable which has n possible discrete outcomes with corresponding probabilities of occurrence p_i. In this situation, the total lack of information can be given by

$$H = -\sum_{i=1}^{n} p_i \log_n p_i, \tag{35}$$

where $\log_n$ is the logarithm to the basis n.

This quantity has the same basic properties of classical statistical entropy given by (34): if any $p_k = 1$, all the others are zero ($\sum_i p_i = 1$) and H equals to zero, which results in a certainty that outcome k will be obtained. On the other hand, when all outcomes are equally likely to occur H achieves its maximum value. Since we choose base n to the logarithm function, this maximum value results to 1. This can be easily proved by substituting $p_i = 1/n$ in (35):

$$H = -\sum_{i=1}^{n} \frac{1}{n} \log_n \left(\frac{1}{n}\right) = n\frac{1}{n} \log_n n = 1. \tag{36}$$

If we associate information to the capacity to predict a single outcome among all these n possible ones, the situation of maximum H can clearly be associated to complete lack of information about which outcome will result, i. e., complete unpredictability. Situations in which $H < 1$ unequal values of p_i, resulting in some degree of predictability, which can be associated to the idea that some information about the outcomes is available. When any $p_k = 1$, all the others are zero and we have certainty that outcome k will result, corresponding to full predictability, which can be associated to the notion that we have complete information about which outcome will result. In this sense, it is reasonable propose that H can quantify the lack of information about the system which produce these outcomes. Thus, we propose the function I, defined as the total amount of information:

$$I = 1 - H = 1 + \sum_{i=1}^{n} p_i \log_n p_i. \tag{37}$$

If we consider binary events ($p_1 + p_2 = 1$), we can consider $p_1 = p$, $p_2 = 1 - p$ and H will be a function of p only. In this case H has a maximum value 1 at $p = 1/2$, being symmetrical around this value of probability. For binary events that are equally likely to occur (e. g. an unbiased coin toss), the outcome is completely *unpredictable*. This corresponds to $H = 1$ and $I = 0$. On the other hand, for low or high values of p (near zero or 1), one event is extremely rare and its counterpart is extremely frequent, regions in which H attains very low and I very high values. In this case, we have very *predictable* events. For $p = 1$ we have $H = 0$ and $I = 1$, corresponding to *certainty*.

The MZI setup produces binary events. The screen 1 receives a photon with probabilities of association to path A or B given by (24) and (25), respectively. On screen 2, these probabilities are respectively given by (27) and (28). We can define functions given by (35) and (37) for each screen from these probabilities, each one depending only on parameters R_1 and R_2. It is straightforward to

show that the lack of path information is given by

$$\begin{aligned} H_{\mathrm{P1}} &= -\,p_{1\mathrm{A}}\log_2 p_{1\mathrm{A}} - p_{1B}\log_2 p_{1\mathrm{B}} \\ &= -\frac{R_2(1-R_1)}{R_1+R_2-2R_1R_2}\log_2\left[\frac{R_2(1-R_1)}{R_1+R_2-2R_1R_2}\right] \\ &\quad -\frac{R_1(1-R_2)}{R_1+R_2-2R_1R_2}\log_2\left[\frac{R_1(1-R_2)}{R_1+R_2-2R_1R_2}\right], \end{aligned} \tag{38}$$

for screen 1, and

$$\begin{aligned} H_{\mathrm{P2}} &= -p_{2\mathrm{A}}\log_2 p_{2\mathrm{A}} - p_{2\mathrm{B}}\log_2 p_{2\mathrm{B}} \\ &= -\frac{R_1R_2}{R_1(2R_2-1)-R_2+1}\log_2\left[\frac{R_1R_2}{R_1(2R_2-1)-R_2+1}\right] \\ &\quad -\frac{(1-R_1)(1-R_2)}{R_1(2R_2-1)-R_2+1}\log_2\left[\frac{(1-R_1)(1-R_2)}{R_1(2R_2-1)-R_2+1}\right]. \end{aligned} \tag{39}$$

for screen 2. The total amount of path information corresponding to each screen is readily obtained by definition (37), resulting $I_{\mathrm{P1}} = 1 - H_{\mathrm{P1}}$ and $I_{\mathrm{P2}} = 1 - H_{\mathrm{P2}}$.

Expressions (38) and (39) are somewhat complicated functions of parameters R_1 and R_2. To visualize them in a simpler way, we made a plot of a 2D contour map of I_{P1} and I_{P2} as a function of R_1 and R_2, as shown in Figure 4. These plots were built using a similar paradigm we adopted to create Figure 4 of our previous work [1]. For each screen, along each correspondent diagonal lines I_{P1} and I_{P2} are zero. For screen 1 (blue contours), the values of R_1 and R_2 which lie along the diagonal line correspond to interference patterns with visibility 1 on this screen (occurring with less visibility on screen 2 for these parameters). Only for $R_1 = R_2 = 0.5$ (both beam splitters balanced) we have $I_{\mathrm{P1}} = I_{\mathrm{P2}} = 0$, resulting in interference patterns with visibility 1 on both screens. Along black horizontal ($R_2 = 0.5$) and vertical ($R_1 = 0.5$) lines we have $I_{\mathrm{P1}} = I_{\mathrm{P2}}$. At the green circles and on its respective screen, I_{P1} and I_{P2} are not defined, because no photons hit this respective screen. At these values of R_1 and R_2 all photons are detected on the other screen. High values of path information are usually characteristic on cases in which $R_1 \cong 1 - R_2$ on screen 1 and $R_1 \cong R_2$ on screen 2 – indeed, in these situations we have high values of respective distinguishabilities.

Let us address now the case in which the first beam splitter is balanced and the second is unbalanced (the black vertical line in both contour plots of Figure 4), making $R_2 = R$ and $T_2 = T = 1 - R$, like we considered in Figure 3. In this case we have $p_{1\mathrm{A}} = p_{2\mathrm{B}} = R$ and $p_{1\mathrm{B}} = p_{2\mathrm{A}} = 1 - R$. Furthermore, visibility and distinguishability are the same on both screens (see Figure 3) and so the amount of path information. It is straightforward to show that

$$\begin{aligned} H_{\mathrm{P1}} &= H_{\mathrm{P2}} = H_{\mathrm{P}} = -R\log_2 R \\ &- (1-R)\log_2(1-R), \end{aligned} \tag{40}$$

which leads to

$$\begin{aligned} I_{\mathrm{P1}} &= I_{\mathrm{P2}} = I_{\mathrm{P}} = 1 + R\log_2 R \\ &+ (1-R)\log_2(1-R). \end{aligned} \tag{41}$$

Figure 5 shows a plot of H_{P} and I_{P} as a function of R, the reflection coefficient of the second beam splitter, compared to $\mathcal{V}^2$ and $\mathcal{D}^2$. It is noticeable that the lack path of information function H_{P} has its behavior very similar to the square of visibility. This is expected, since the larger the lack of path information, the larger the

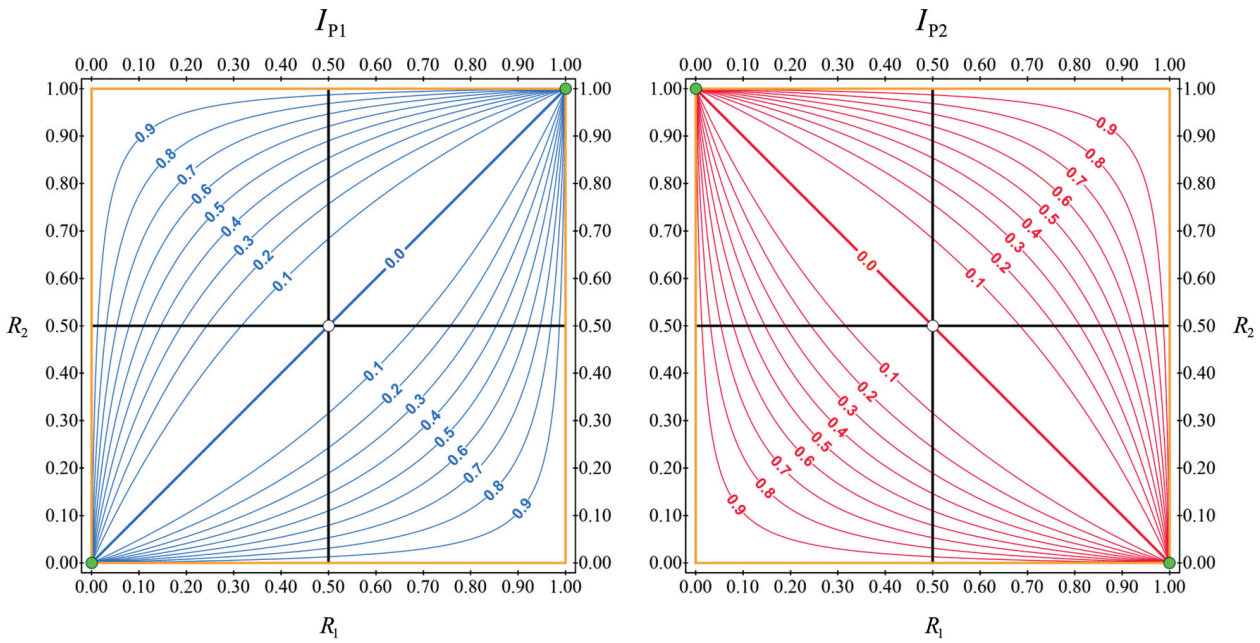

Figure 4: Contour plots of total amount of path information on both screens – I_{P1} (screen 1, in blue) and I_{P2} (screen 2, in red) – as a function of R_1 and R_2. Both are maximum simultaneously over the orange border (equals to 1), except at the corner points (green circles), where only one of them vanishes and the other is not defined.

 DOI: http://dx.doi.org/10.1590/1806-9126-RBEF-2019-0283

contrast of interference pattern. Thus, it is reasonable propose H_P or $\mathcal{V}^2$ as measure of the degree of wave-like behavior of photons in the interferometer. Conversely, the behavior of the amount of path information function I_P is very similar to $\mathcal{D}^2$, being also reasonable to propose both as a measure of the degree of wave-like behavior of the photons in the interferometer. At $R = 0.5$ (both beam splitters balanced), $H_P = 1$ and $I_P = 0$, i. e., photons exhibit a pure wave-like behavior. For $R = 0$ or $R = 1$, $H_P = 0$ and $I_P = 1$, which corresponds to a pure particle-like behavior.

Although functions formally similar to (35) have been proposed mainly to quantify lack of information, their use does not restrict to this concept. Entropy-like functions can be used as a measure of *diversity* of a categorical variable in a sample (e. g., representing ethnic distribution, socioeconomical levels, different kind of species in an environment and others) in which the probabilities are changed to respective proportions of elements or individuals that belong to each category. Indeed, similar functions in statistics have been proposed to accomplish this task [84].

3. Part II: The software in quantum picture and a teaching example

In this section, we will present some essential features of VMZI followed by analysis of discursive interactions among students' (pre-service physics teachers) in didactical situations mediated by this software. These didactical activities were focused on topics which has been discussed in sections 2.2 and 2.3.

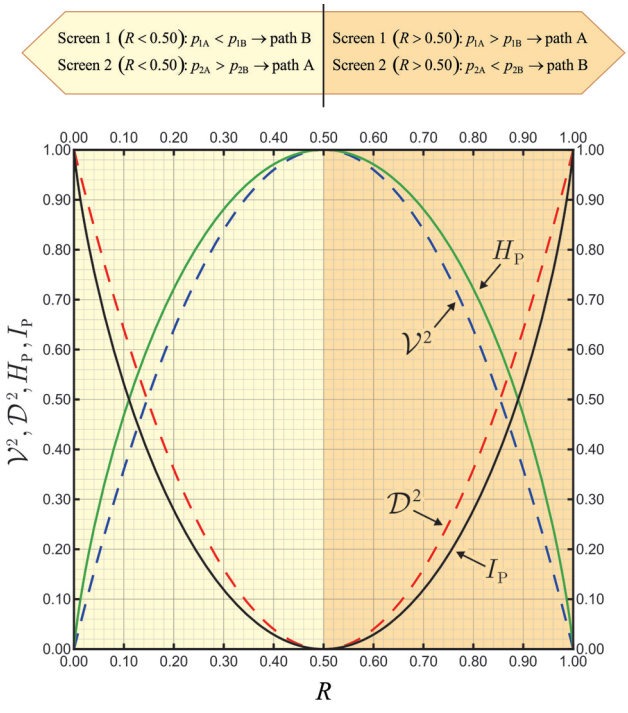

Figure 5: Plot of $\mathcal{V}^2$, $\mathcal{D}^2$, H_P, and I_P as a function of R considering the first beam splitter is balanced. The second beam splitter is unbalanced with $R_2 = R$ and $T_2 = T$. For all range the H_P and I_P functions are close to $\mathcal{V}^2$ and $\mathcal{D}^2$, respectively.

3.1. A brief description of the software in quantum picture

In Figure 6 a screen is shown a capture of VMZI interface (labelled as 1). The interface is composed by widgets, each one designed with its specific purpose. In widget 2, we show how the classical (option Laser) or quantum (option Single Photons) pictures of interferometer can be selected – dropdown options are shown in detail in 3. Also, in widget 2, input values of some parameters (e.g. R_1 and R_2) can be chosen.

These parameters are related to devices which are present or can be placed at the interferometer arms: two beam splitters, detectors or polarization filters (remembering, last two are not addressed in this paper). Numerical values of interference visibility in each screen appear in the bottom of this widget. In widget 4 all possible photon counts are provided, showing theoretical predictions and results of simulations (basically performed using a weighted random choice algorithm), including path distinguishability in each screen. Widget 5 shows some interface settings related to visualization of VMZI and the language option (currently Portuguese and English are available).

It is worth to highlight to students the probabilistic nature of photon incidence on each screen. To stimulate the discussion of this important physical aspect of quantum interference in two-way interferometers like MZI, one can propose that the users, students or teachers, execute three different runs of the software for the same values of all parameters. It is possible to configure the software to stop when a determined number of photons, predefined by the user, is emitted by the source – when this option is active, the maximum quantity allowed is one million photons. They can be configured to be emitted one by one or in pulses of more photons, significantly accelerating the process. These pulses are not meant to describe a real phenomenon (real photon sources) – they are thought to provide a didactical resource to complete the simulation more quickly (we do not expect that users would like to take hours until all photons reach the screens).

To illustrate the probabilistic nature of the interaction between photons and beam-splitters, we performed three different runs of one million photons. The outcomes obtained (the photon counts) are shown in Figure 7.

It is obvious the probabilistic nature of the phenomenon, since different counts were obtained, although relative frequencies in each screen match very well to theoretical predictions, given by $R_1T_2 + R_2T_1$ (on screen 1) and $R_1R_2 + T_1T_2$ (on screen 2) – *N1/NF (simul.)* and *N2/NF (simul.)* fields on the widgets exhibit values almost equal to *N1/NF (theory)* and *N2/NF (theory)* fields.

This happens due to the very large number of photons emitted. The probabilistic nature of the process prevents that these three runs reproduce exactly the same counts.

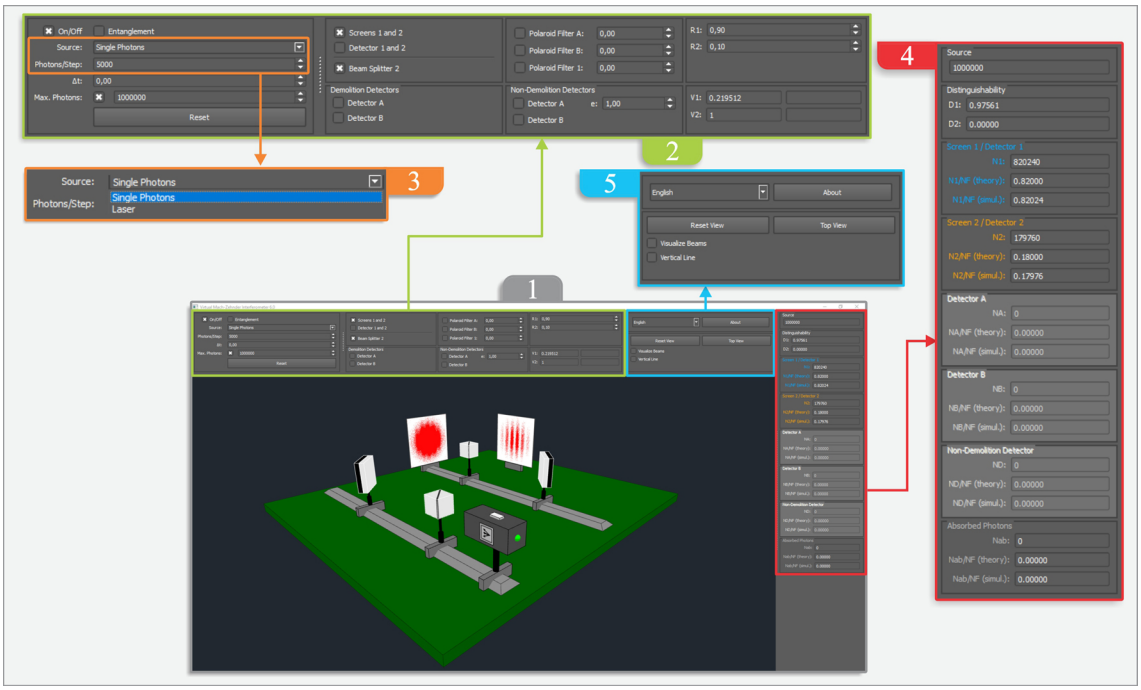

Figure 6: Screen capture of VMZI. The interface contains three main widgets (labelled as 2, 4 and 5), each one designed to different purposes, as explained in the text.

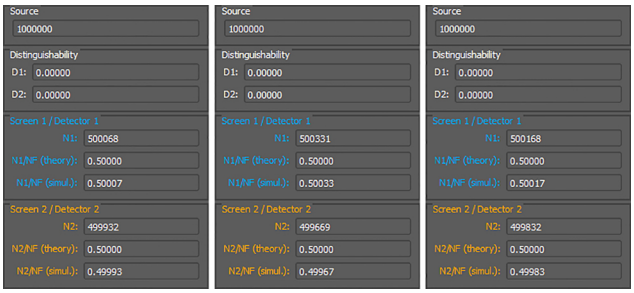

Figure 7: Three different counts on the screens, obtained from the simulation when $R_1 = R_2 = 0.5$, illustrating the probabilistic nature of the reflection and transmission events on the beam splitters.

No matter how many runs are executed, these counts tend to be slightly different, even when the number of photons emitted by the source is large enough.

3.2. Teaching episode

Here we present an excerpt of a didactical activity which took place in an undergraduate physics course of a Brazilian federal institution, involving pre-service physics teachers. The students worked in pairs and are asked to explore the software assisted by the teacher and aided by a didactic guide, in which activities were proposed. They were previously submitted to an introductory course before being engaged in activities with VMZI, in which some fundamental concepts were taught: quantum states, quantum states superposition, probability amplitudes and probability, basics of Dirac's formalism and abstract representation of a quantum state (state vector), quantum operators, observables, eigenvalues and eigenstates, among others. The concept of visibility and distinguishability intentionally were only taught along the didactical activity with the software. Our intention was to let students construct discursive strategies to construct reasonings to understand these quantities, present on the software, for posterior analysis.

This course, written notes, along with exploratory guides and teacher's interventions during activities, had an important role on semiotic mediation, crucial to establish and hold intersubjectivity in favor to provide a kind of initial "tuning" process among teacher and students. As shown in the work of Sawyer and Berson [85], the course, written notes and the exploratory guides act as *external representations* and improve significantly the collaborative work. They provide several ways of semiotic mediation, which enriches discursive interactions among students even in absence of teacher assistance (e.g., in study groups). In discursive interactions, students often revoice all kinds of course material (teacher speeches, written notes and others) with their own words, which in turn enriches the discussion about physical phenomena involved, stimulating new insights and routes for dialogical learning. Students' utterances were recorded in audio and video for posterior analysis. Our perspective focus attention more in the processual analysis of group interactions (mainly discursive interactions) than in initial and final educational outcomes (e.g. tests results). Although this premise does not exclude the importance of educational outcomes provided by tests or similar as auxiliary data, these outcomes alone do not effectively

capture discursive learning strategies which occur along didactical interventions that privilege collaborative work among peers. As stated by Hicks [86, p. 136], we assume that learning manifests as "the coconstruction (or reconstruction) of social meanings from within the parameters of emergent, socially negotiated, and discursive activity". Coherently with this perspective, students' speeches are our primary source of data to be analyzed.

In the first activity, students are asked to set beam splitters' coefficients to $R_1 = R_2 = 0.5$. The following questions were proposed:

- *What can we say about the quantum translational state of the photon after the first beam splitter? What is the path associated to it?*
- *How can we explain the formation of these figures on the screens?*

Figure 8 shows this situation in the MZI. A pair of students (Augusto and Carlos) ran the simulation activity on the VMZI with these parameters and produced the following utterances (text between brackets was inserted by us to clarify what students meant).

1. *Carlos: We can't conclude anything by looking at the first [beam] splitter here.*
2. *Augusto: Yes, it can follow both ways.*
3. *Carlos: The interference pattern is very clear.*
4. *Augusto: Yes, it has visibility 1.*
5. *Carlos: But it does not help, because you know nothing about the [path associated to the] photons.*
6. *Augusto: You can only say that you have a 50 percent chance on each path. It's the same as knowing nothing [about the path].*
7. *Carlos: It is unpredictable. It can be either one path or the other. As with slits, it can pass through one or another slit.*

To explain the interference, they were instructed to consider the phase difference φ introduced by the possible paths associated to the photon in the MZI, each of these paths ending in a particular point x of the screens. However, here the focus was on the relation between the available path information and visibility of interference patterns (this is why the dialogue above develops through these two concepts). They understood the formation of interference patterns in this situation and that maximum visibility leads to no path information at all. In other words, they understood that the photons exhibit a pure wave-like behavior.

The students established a direct relationship between the simulation on the VMZI and the double-slit experiment when two beam splitters are balanced (inability to infer about which slit the photon passed through, considering the quantum picture). The equivalency of MZI and the double slit system is discussed in Cavalcanti, *et al.* [1] considering the classical picture. Additionally, the probabilities mentioned in the utterance 6 and implicitly in utterance 2 (referring to the first beam splitter) are related to the predictability $\mathcal{P}$ (null in this case) – at this point the distinguishability $\mathcal{D}$ was not cited. They were not aware about how the second beam splitter affects the visibility of the interference pattern. This is already expected in the early stages of the initial simulation activities with the VMZI, so that the analogies that students make with the double-slit experiment fall on the visually more obvious aspects to be perceived: the formation of interference patterns with full visibility and no path information available. There is no sign of discontent of the students about the results obtained at this early stage, as it seems natural to get an interference pattern in an experiment like this. It is necessary to bring some counterintuitive feature to lead them into a deeper discussion

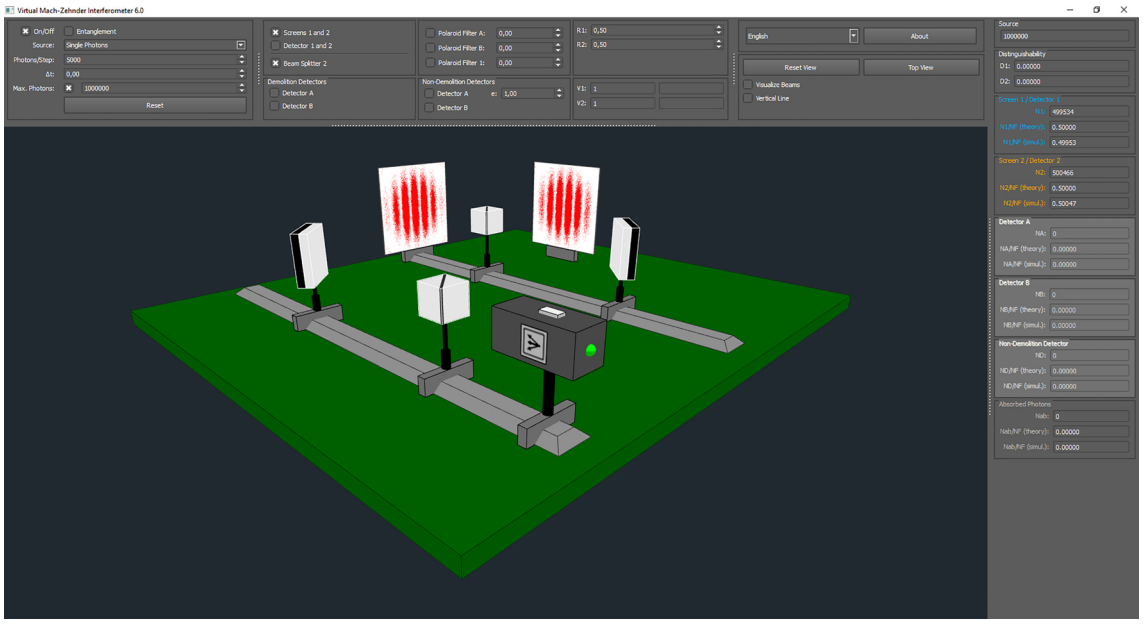

Figure 8: Interference patterns formed on the screens when the beam splitters are balanced ($R_1 = R_2 = 0.5$).

of the quantum interference. In this case, the visibility on each screen is equal to unity and no path information is available, as can be obtained from equations (12) and (13). The maximum contrast interference patterns were built by one million photons, approximately half million hitting each screen.

As stated above, when students argue about the impossibility of inferring the path associated with the photon in the interferometer after the interaction with the first beam splitter, they are referring to the fact that predictability $P = |R_1 - T_1|$ is null because $R_1 = T_1$. This implies, from equation (17), that there is a probability of 50 percent of successfully guessing the path after the first beam splitter. The translational state of the photon just after BS_1 (and before interacting with the mirrors) are transformed into a superposition of two possible translational states $|s_x\rangle$ and $|s_y\rangle$:

$$|\Psi_{\text{in}}\rangle = |s_x\rangle \xrightarrow{\hat{\mathbf{S}}_1\ (\text{first beam splitter})} |\Psi^{\text{I}}_{\text{BS}_1}\rangle$$
$$= \text{i}\sqrt{R_1}|s_y\rangle + \sqrt{T_1}\,|s_x\rangle = \frac{1}{\sqrt{2}}\left(\text{i}|s_y\rangle + |s_x\rangle\right). \quad (42)$$

The state given by (42) shows that the probabilities for a photon to be measured in arm A or B are both equal to 0.50. Although the student Carlos uses the word "unpredictable" to refer to the limitations imposed by this probability distribution (utterance 7), it cannot be taken for granted that he was really aware about the notion of predictability as discussed here. It is a sort of informal language, at most an implicit reference to this concept to express the idea that any of the two events (reflection or transmission) can occur with equal probability, as shown in equation (42), and that it would be impossible to obtain prior information about which one will occur. Maximum visibility implies null distinguishability on both screens, as predicted by the complementarity relation expressed in equation (15). This situation is one of the extreme cases considered by Bohr, in which no path information is available, corresponding to a pure wave-like behavior.

The opposite extreme situation can be explored through computational simulation in multiple ways, as stated before. The following utterances refer to a simple parameter combination that results in an extreme case in which $V_1 = V_2 = 0$. Here, the students were asked to remove the first beam splitter, which is equivalent to set $R_1 = 0$. The following questions were asked:

- *What changes would occur on the screens while maintaining $R_2 = 0.5$, but removing the first beam splitter (make $R_1 = 0$ to explore this option)?*
- *How would you explain the outcomes on both screens?*

The following utterances were produced:

8. *Augusto: The probability is not 50 percent anymore. It is 100 percent.*
9. *Carlos: All the photons are transmitted and come right here [arm A].*
10. *Augusto: Look, the interference has gone. The visibility decreased to zero.*
11. *Carlos: Naturally, now we are sure that the photon goes to that way.*
12. *Augusto: At least until the photon reaches the second [beam] splitter, then it gets unpredictable again.*
13. *Carlos: Yes, this is why the figure gets blurred on both screens.*

In this case, the predictability is 1 (utterance 8), that is, students can infer with certainty, in advance, that all photons will remain in the translational state $|s_x\rangle$ after their interaction with BS_1.

No interference pattern was observed on the screens (see Figure 9). It is important to note here that students have satisfactorily analyzed the translational state of the photon (utterance 9) and explicitly considered the role played by the second beam splitter (BS_2). However, there is a subtle statement in utterance 12 that induces a *potential* confusion in utterance 13, which can lead to an oversimplification of the role of the second beam splitter. Augusto starts saying *at least until the photon reaches the second [beam] splitter*, suggesting that if the second beam splitter is balanced, then the path information (here inserted by configuring BS_1 as totally transparent) could be somehow erased. Carlos brings extra confusion saying that is BS_2 chosen as balanced that causes interference to vanish. His expression of confusion suggests that the activity allowed students to face the internal contradiction in their own reasoning, realizing the necessity of a better articulated narrative. In this situation, there is full path information available on the translational state of the photons (considering both screens), due to full transmissivity (or absence) of the first beam splitter ($R_1 = 0$, $T_1 = 1$). In this situation, all photons detected at the output ports are associated with path A (see Figure 1), which results in distinguishability 1 for both screens. This distinguishability, however, cannot be confused with the probability of inferring correctly the path associated to any photon that hits each screen. This probability is given by $P_{1\text{ms}} = (1 + \mathcal{D}_1)/2$ and $P_{2\text{ms}} = (1 + \mathcal{D}_2)/2$, both equal to 1 (as the distinguishabilities), i.e., the second beam splitter in no way makes unpredictable the path associated with each photon. In the case analyzed, it is known that all the photons registered on screen 1 were reflected in BS_2 and photons registered on screen 2 were transmitted by that device. The "unpredictable" attribute used by the student Augusto refers to which of two events (reflection or transmission) will occur after interaction of the photon and BS_2, not to the path (A or B) associated to each photon that hits the screens. The state of the photon at the output ports of the interferometer in this case can be obtained from equation (9) and is given by

$$|\Psi_{\text{out}}\rangle = -\frac{\text{i}}{\sqrt{2}}\text{e}^{\text{i}\varphi}\,|s_x\rangle - \frac{1}{\sqrt{2}}\text{e}^{\text{i}\varphi}|s_y\rangle$$
$$= -\frac{1}{\sqrt{2}}\text{e}^{\text{i}\varphi}\left(\text{i}\,|s_x\rangle + |s_y\rangle\right). \quad (43)$$

 DOI: http://dx.doi.org/10.1590/1806-9126-RBEF-2019-0283

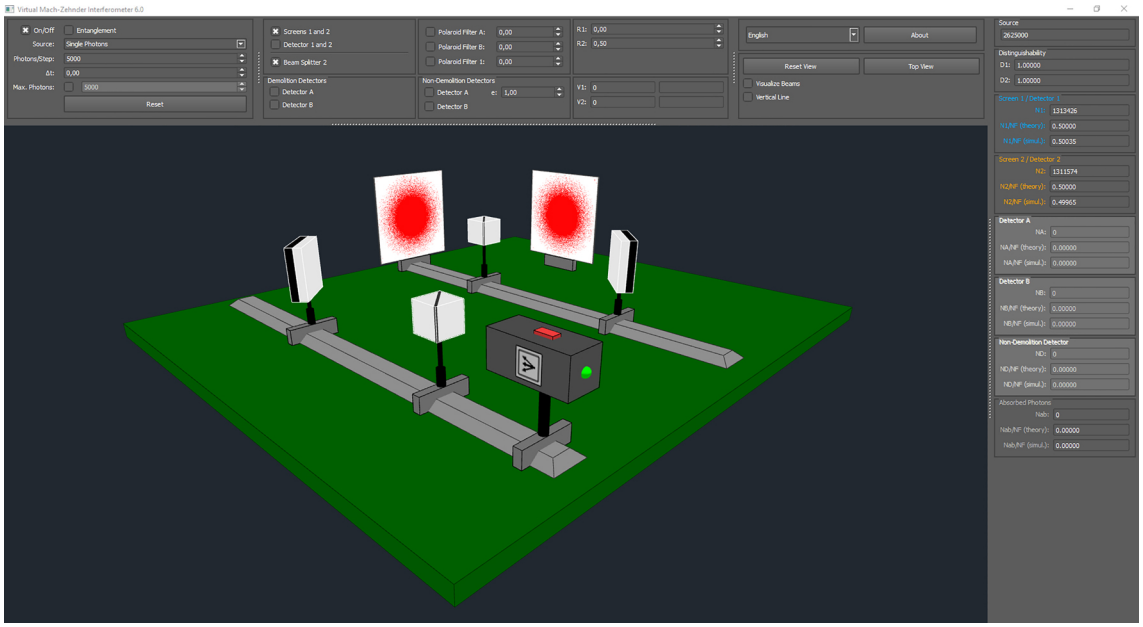

Figure 9: When $R_1 = 0$, no interference pattern appears on the screens. Here, the second beam splitter is balanced ($R_2 = 0.5$).

It is clear that no interference occurs on both screens. Furthermore, note that the state described by (43) has only a global phase φ. However, the probability that a photon exits by output port 1 hitting the screen 1 is 0.5, the same happening on screen 2. The port from which the photon emerge is really *unpredictable*, but, regardless this fact, the path associated to the photon is always path A and no interference pattern will arise on any screen – choosing BS_2 as balanced will not erase path information, in this situation inserted by removal of BS_1 or setting it as totally transparent ($T_1 = 1$). This scenario is similar (but not exactly the same) as that obtained with $R_2 = 0$ (equivalent to remove BS_2) and $R_1 = T_1 = 0.5$, shown in Figure 10. In this case, the available path information is due to BS_2 absence, not to BS_1. The translational state of the photon after BS_1 (before interacting with the mirrors in each arm) is represented in equation (42) and results in null predictability, as we have $R_1 = T_1$. In other words, the "unpredictability" is transferred to BS_1. On the other hand, since BS_2 is absent, the final translational state will be given by:

$$\begin{aligned} |\Psi_{\text{out}}\rangle &= -\mathrm{i}\sqrt{R_1}\,|s_x\rangle - \mathrm{e}^{\mathrm{i}\varphi}\sqrt{T_1}|s_y\rangle \\ &= -\frac{1}{\sqrt{2}}\left(\mathrm{i}\,|s_x\rangle - \mathrm{e}^{\mathrm{i}\varphi}|s_y\rangle\right). \end{aligned} \tag{44}$$

All photons with translational state $|s_x\rangle$ immediately after BS_1 (photons associated with arm A) will be detected in screen 1 and all those whose translational state is $|s_y\rangle$ after BS_1 (photons associated with arm B) will be detected on the screen 2. Because full path information is available, no interference pattern appears on screens.

Thus, the vanishing of interference patterns is not due to the "unpredictability" of what happens after the photon interacts with BS_2, as pointed by student Augusto (utterance 12) and wrongly interpreted by Carlos as the cause of destruction of interference pattern (utterance 13). It is also important to point out again that the probability of inferring correctly the path taken by any photon detected on each of the screens is 1, since the distinguishability is also 1 (is the full path information available that destroys the interference patterns).

The activity with two beam splitters configured as jointly balanced (utterances 1 to 7) can help to construct the notion that the unpredictability of what happens after the interaction between the photon and them is a necessary attribute to obtain interference patterns with visibility 1 in the MZI (on both screens). Students were moderately comfortable with the results of the first activity, as we can see in utterances 1-8. When they set only the second beam splitter as balanced and the first totally transparent, some confusion arises (specially for Carlos, on utterance 13). This strategy is intentionally adopted to force discussion about the role of the beam splitters on the formation of interference patterns when studying complementarity, stressing the fact that their role goes beyond the introduction of a $\pi/2$ phase difference between transmitted and reflected photon or the transformation of initial translational state $|s_x\rangle$ into a superposition given by (42). They can be configured by means of parameters R_1 and R_2 to determine *a priori* (BS_1) and *a posteriori* (BS_2) path information, which results in changes on the visibility of interference patterns. When $R_1 = 0.5$, this specific role of both beam splitters is not obvious to most of students and can be brought to discussion only when R_1 and R_2 can be freely changed. Even in the case of perfectly balanced beam splitters, their role on interference phenomena can be not obvious to students [87]. Despite these difficulties, the students understood quite satisfactorily that pho-

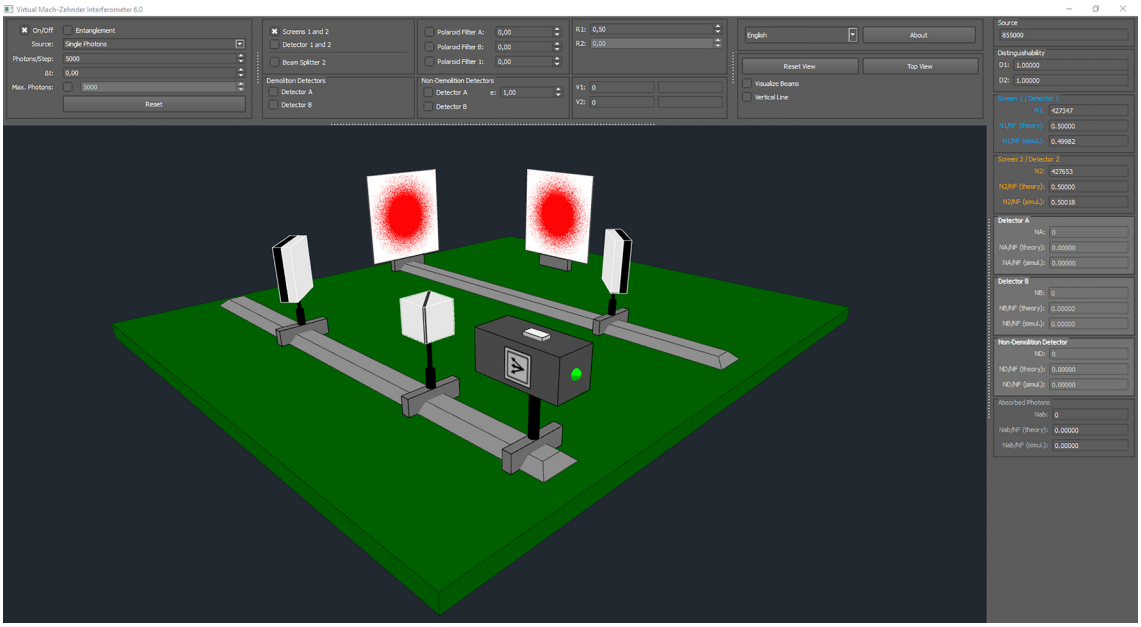

Figure 10: No interference pattern appears on the screens when first beam splitter is balanced and the second is removed (it is equivalent to set $R_1 = 0.5$ and $R_2 = 0$).

tons exhibit pure particle-like behavior in the situation represented on Figure 9.

The next activity was conceived to emphasize the role of the second beam splitter and introduce intermediary interference, by means of a situation in which the coexistence of particle-like and wave-like behaviors is remarkable. To do so, as we show in Figure 11, we introduce the context in which the second beam splitter is highly unbalanced (with reflection and transmission probabilities chosen as $R_2 = 0.9$ and $T_2 = 0.1$) and the first is balanced. The following questions were asked:

- *How the interference figures behave?*
- *How can we explain the path associated to the photons?*

We asked the students to explain the change in interference patterns (compared with the one obtained when both beam splitters were balanced) and about the path distinguishability. This is the situation highlited in Figure 3 by the points a, b and c, which indicate, respectively, the probabilty of gessing photon path, given by $P_{\rm ms} = (1 + \mathcal{D})/2$, distinguishability $\mathcal{D}$ and visibility $\mathcal{V}$.

As discussed earlier, this situation produces intermediary interference phenomenon. In this case there is appreciable contrast (discernible interference pattern), but simultaneous and equally significant available ammount of path information (high distinguishability). This situation is a key one (not the only one), obtained for $R_1 = 0.5$ and $R_2 = 0.9$ and highlited in Figure 3 by the points a, b and c, which indicate, respectively, the maximum probabilty of gessing photon path, given by $P_{\rm ms} = (1 + \mathcal{D})/2$, distinguishability $\mathcal{D}$ and visibility $\mathcal{V}$. In this case, interefference patterns are clear (but not so clear as the one shown in the Figure 8), as can be seen in Figure 11, and the probability of guessing the photon's associated path is very high ($P_{1\rm ms} = P_{2\rm ms} = (1 + 0.8)/2 = 0.9$).

14. *Carlos: Wow! Now the two figures are mixed up.*
15. *Augusto: But you cannot tell which path the photon took.*
16. *Carlos: Until the photon reaches the second [beam] splitter we do not know anything, and then even worse, because the [beam] splitter messes everything up and it becomes unpredictable again.*
17. *Augusto: But it is not unpredictable here [after the second beam splitter]! We know that it reflects 90 percent.*
18. *Carlos: Yes, but this reflection [referring to the first beam splitter] injects the same number of photons to one way or another.*
19. *Augusto: But now the distinguishability is no longer zero. Then you must be able to guess the path.*
20. *Teacher: If you chose any photon that was detected on screen 2, for example, could you tell me which path it took?*
21. *Carlos: I do not know, because half of the photons go to each path.*
22. *Augusto: This seems confusing, because the distinguishability is 0.80, but I do not know how we can estimate such probability.*

When $R_1 = 0.5$ and $R_2 = 0.9$, the pattern visibility is 0.6 and the complementarity relation (15) tell us that this visibility leads to a distinguishability of 0.8, a high value. Students may be surprised if they are faced up with the Bohr's complementarity principle as it usually appears in textbooks, dealing only with two extreme situations. It

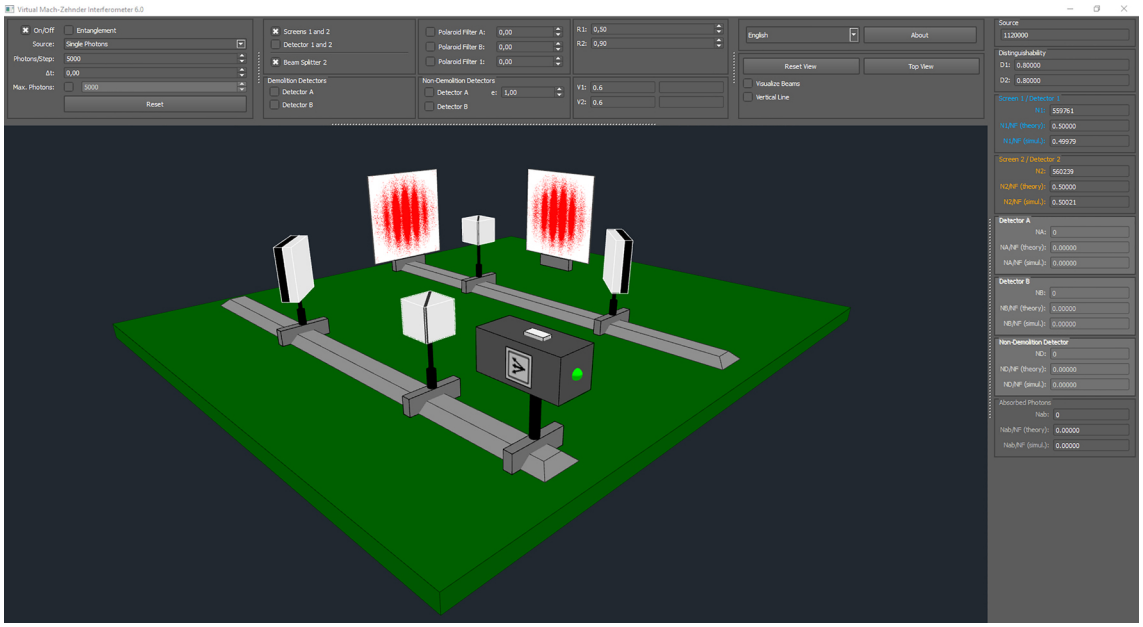

Figure 11: Interference pattern obtained with $R_1 = 0.5$ and $R_2 = 0.9$. Despite the high value of distinguishability (0.8), the probability of correctly guess the path associated to the photon is very high (0.9).

is possible to face situations like that presented here, in which coexists both wave-like and particle-like behaviors.

This surprise seems to have been manifested by Carlos, who says *the two figures are mixed up* (clear interference and no interference superposed, resulting in blurred interference patterns), although Augustos' concern to infer the path associated the translational state of the photon was the central point of the discussion between them. Carlos become confused with the role of the second beam splitter in utterance 16. He correctly interprets the impossibility to infer the path associated to the photon when it interacts with the first beam splitter (null predictability), but erroniously atributes unpredictability to the second beam splitter ([...] *because the [beam] splitter messes everything up and it becomes unpredictable again*). Augusto understood better the role of the second beam splitter in this situation (it encodes path information in the translational state of the photon), correcting Carlos in utterance 17. Carlos shows resistance to accept that the second beam splitter provides path information here (utterance 21), even after teacher intervention (a question asked in utterance 20). Even with a better comprehension than Carlos about the role of the second beam splitter, Augusto does not know how to estimate the probability of guessing right the path associated with any phtoton that hits screen 2, but he was aware that this probability is not the same thing as the distinguishability.

The "mixture" referred in utterance 14 by Carlos – intermediary interference, i.e., coexistence of particle-like and wave-like behaviors – does not violate the complementarity principle. Generalization of this principle take into account partial interference, restricting visibility and path information by complementarity equation (15) as in the present situation. Equation (14) is more general and is valid when the translational state of the photon cannot be described by a coherent superposition like (9) (this can happen when the photon is prepared in a mixed translational state – this would require substitution of the first beam splitter by a more complex device). The probability of correctly guessing the path associated to the photon here is remarkably high (0.90, considering that our guess is path A for screen 1 or path B for screen 2).

The next situation was not originally included in the exploratory guide. It was introduced from a question asked by a student after he ends the previous situation, described above. The student asked "what happens to the interference patterns if we choose a very low value to R_1 and a very high value to R_2?".

Staring from this good question, we designed a very interesting situation. It is shown in Figure 12, and obeys the condition $R_1 + R_2 = 1$. Making $R_2 = 1 - R_1$ in equation (13), it is straightforward to show that $\mathcal{V}_2 = 1$ and $\mathcal{V}_1 < 1$, if we have $R_1 \neq 1$ and $R_1 \neq$ (if R_1 assumes one of these two values we obtain extreme situations in which visibility is zero and distinguishability is 1). Almost extreme values like $R_1 = 0.02$ and $R_2 = 1 - R_1 = 0.98$ cause very blurred and undiscernible interference pattern on screen 1 (the visibility is approximately 0.041 and distinguishability is 0.999) and a perfect pattern (visibility 1) on screen 2, but with a very low number of photons hitting this screen if compared with the number of photons that hit screen 1. The students produced the following utterances:

23. *Carlos: Now I am completely confused. First, we got a clear interference pattern. Then we changed the coefficients and the patterns became blurred.*

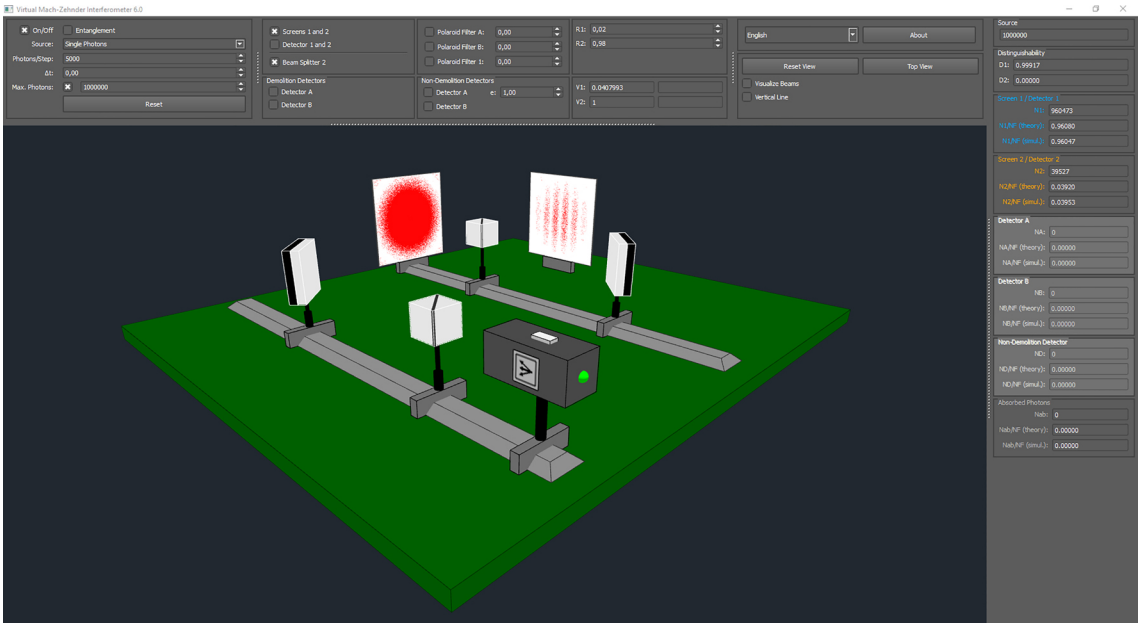

Figure 12: Interference pattern obtained with $R_1 = 0.02$ and $R_2 = 1 - R_1 = 0.98$. A very blurred interference pattern arises on screen 1 while a visibility 1 pattern arises on screen 2.

And now we see this [very blurred on one screen, full visibility on the other]!

24. *Augusto: I think it is weird too, but now I would venture to say that most of the photons were transmitted and then reflected.*
25. *Carlos: Now there is a lot of [path] information available here. The first beam splitter causes this. But I cannot understand how different figures can arise on two screens.*
26. *Augusto: The more the [path] information available, the more blurred the figure. Have you seen that the interference pattern has diminished [it becomes faint on screen 2, although visibility is 1]?*
27. *Carlos: Yes, they keep changing [as running simulation], but it does not make sense.*
28. *Augusto: Previously we had just wave or particle. Now it is wave-particle. I'm just in doubt about the probability. This is not unpredictable anymore, because you can know very well what will happen after BS_2.*
29. *Carlos: I think I am not understanding anything!*

Both Carlos and Augusto use the notion of path information in utterances 25 and 26, relating it directly with the visibility of interference pattern. Since path information and distinguishability (and also *lack* of path information and visibility) are closely related quantities, qualitatively this is not a problem (see Figure 5). This situation generated confusion, which is what we expected. Considering each beam splitter individually (both have almost extreme values of reflection coefficients), they seem to consider natural to conclude that there is considerable amount of path information in this situation, since the photons are almost certainly transmitted by the first beam splitter ($T_1 = 1 - 0.02 = 0.98$) and almost certainly reflected by the second ($R_2 = 0.98$). They remain comfortable with the observed interference patterns on screen 1 but confused when they observe what happens on screen 2. Carlos states this confusion in utterance 23, with which Augusto agrees (utterance 24). In this utterance, Augusto identifies the source of confusion (*I would venture to say that most of the photons were transmitted and then reflected*) – is clear that is much more likely to occur transmission when photon interacts with beam splitter 1 and reflection when it interacts with beam splitter 2, but Augusto is not aware that this reasoning is very problematic. Both students consider each beam splitter individually but is their joint action on translational state of the photon that defines visibility of interference patterns (and also the distinguishability). Carlos states explicitly that he did not understand *how different figures can arise on two screens* (utterance 25) and Augusto follows this assertion reinforcing the notion that the more the path information available, the more blurred the interference pattern (utterance 26). He reinforces this idea on utterance 28 (*This is not unpredictable anymore, because you can know very well what will happen after BS_2*), thinking the interference phenomena only in terms of the action of the second beam splitter, which he considers producing very predictable outcomes.

This situation is very rich to stress the importance on considering both beam splitters in an articulated way – thinking only by means of their individual reflection probabilities leads to misleading interpretations. On the end of this episode, Augusto raise another important question in the beginning of utterance 28 (*Previously we had just wave or particle. Now it is wave-particle.*): would not the wave-like and particle-like behaviors of photons be mutually exclusive? Carlos answers this statement

saying that he cannot understand the outcomes on both screens. They are referring about formation of a very blurred interference pattern on screen 1 (almost pure particle-like behavior) and pattern with maximum on screen 2 (pure wave-like behavior), which seems difficult to explain in the light of the complementarity relation (15). However, this is a false violation of complementarity principle, because the MZI is equivalent to two double slits experiments, one for each screen [see 1, Figure 2]. Thus, complementarity relation is strictly valid only on each experiment, i.e., on each screen. Indeed, by using polarization filters it is possible to obtain pure particle-like behavior on one screen and pure wave-like behavior on the other (the quantum eraser experiment) – this does not violate complementarity principle. This emphasizes the importance of knowing in detail how MZI works, going beyond what physics textbooks usually do. The VMZI can be valuable if articulated in a didactic project in order to promote rich discussions about this kind of subtleties. Although students evinced some difficulty in concepts relating to visibility, distinguishability or probability of correctly inferring the path associated to any detected photon, the simulation helps them to think about subtle aspects of interferometric complementarity, since it brings up rich context to debate, which provides an equally rich ground to teacher later discuss in detail the role of beam splitters and several aspects addressed right above. This type of approach can be very helpful to reinforce the notion that the wave and particle characters are exclusive even if both particle-like and wave-like behaviors are exhibited, each one on a different screen. This is why we dedicated special attention on initial statement contained in utterance 28.

This last didactical situation can be used also to discuss concept of visibility as *contrast*, despite the name *visibility* could be (erroneously) interpreted as *capacity to see* the interference pattern. In expressions (20), the probabilities that a photon reaches any point on the screen 1 or 2 are given, respectively, by $P_{S1} = R_1T_2 + R_2T_1$ and $P_{S2} = R_1R_2 + T_1T_2$. When $R_1 + R_2 = 1$ these probabilities are transformed into $P_{S1} = 2R_1(R_1 - 1) + 1$ and $P_{S2} = 2R_1(1 - R_1)$. So, on screen 1 the probability of incidence is approximately 0.96 (more precisely 0.96080), being approximately 0.04 (more precisely 0.03920) on screen 2 – these are the theoretical predictions *N1/NF (theory)* and *N2/NF (theory)* shown in the photon counts widget. This obviously leads to much fewer photons hitting screen 2 than screen 1, forming a weak (few punctual marks if compared to screen 1) interference pattern on the former. However, although this pattern can be *difficult to see*, it is a very sharp interference pattern, since its visibility is 1. The simulation shown in Figure 12 produced the following outcomes (for 10^6 photons emitted by the source): 960473 photons hit screen 1 (approximately 96 percent of total) and 39527 hit screen 2 (approximately 4 percent of total). Although a low number of photons hit screen 2, a sharp interference pattern is formed (even though it is difficult to *see* it). When we choose $R_1 = 0$ or $R_1 = 1$, we obtain $P_{S1} = 2R_1(R_1 - 1) + 1 = 1$ and $P_{S2} = 2R_1(1 - R_1) = 0$, i.e., all emitted photons reach screen 1 and there is no incidence on screen 2 (in this case, visibility is not defined on this screen).

It is possible to produce a similar situation to that depicted in Figure 12 choosing $\mathcal{V}_1 = 1$ and $\mathcal{V}_2 < 1$ when $R_1 = R_2$ ($R_1R_2 \neq 1, 0\}$). In this case, expressions (20) and (21) lead to $P_{S1} = 2R_1(1 - R_1)$ and $P_{S2} = 2R_1(R_1 - 1) + 1$, reversing the interference pattern and probabilities of incidence on screen 1 if compared to the situation shown in Figure 12. Other situations allow to explore interferometric complementarity, such as insertion of non-demolition detector with configurable efficiency or polarization filters. We plan to explore these more complex situations in a future work.

4. Conclusions

The simulations performed using VMZI presented here where conceived to address one of the most current and culturally rich topics of quantum physics, the wave-particle interferometric complementarity. The discussion about the concepts of predictability and distinguishability goes beyond what is traditionally seen in most textbooks and courses. This kind of approach can help to innovate the teaching of complementarity and appears as an alternative to its study in a more current perspective. This approach can be taught both qualitatively and quantitatively, and therefore we have chosen to discuss some important aspects of the mathematical formalism involved. Dirac's formalism, which is quite abstract for those unfamiliar with quantum physics, acquires more meaning when it is used, for example, to represent the action of the interferometer devices from operators or to calculate probability amplitude on screens. The MZI can be a valuable context to discuss the interplay between mathematical formalism and phenomenology of key aspects of quantum physics.

Acknowledgments

The authors acknowledge the Brazilian National Council for Scientific and Technological Development for the financial support that has been fundamental for the development of this research.

References

[1] C.J.H. Cavalcanti, F. Ostermann, N.W. Lima and J.S. Netto, European Journal of Physics **38**, 065703 (2017).
[2] K. Krijtenburg-Lewerissa, H.J. Pol, A. Brinkman and W.R. van Joolingen, Physical Review Physics Education Research **13**, 010109 (2017).
[3] E. Marshman and C. Singh, Physical Review Special Topics - Physics Education Research **11**, 020119 (2015).
[4] C. Singh and E. Marshman, Physical Review Special Topics - Physics Education Research **11**, 020117 (2015).
[5] C. Singh, American Journal of Physics **76**, 400 (2008).

[6] G. Zhu and C. Singh, American Journal of Physics **79**, 499 (2011).
[7] A. Kohnle, D. Cassettari, T.J. Edwards, C. Ferguson, A.D. Gillies, C.A. Hooley, N. Korolkova, J. Llama and B.D. Sinclair, American Journal of Physics **80**, 148 (2012).
[8] A. Kohnle, I. Bozhinova, D. Browne, M. Everitt, A. Fomins, P. Kok, G. Kulaitis, M. Prokopas, D. Raine and E. Swinbank, European Journal of Physics **35**, 015001 (2014).
[9] G.E.M. Cabral, A.F. de Lima and B. Lula Jr., Revista Brasileira de Ensino de Física **26**, 109 (2004).
[10] T.L. Dimitrova and A. Weis, European Journal of Physics **31**, 625 (2010).
[11] E. Marshman and C. Singh, European Journal of Physics **37**, 024001 (2016).
[12] C. Ferrari and B. Braunecker, American Journal of Physics **78**, 792 (2010).
[13] E.J. Galvez, American Journal of Physics **78**, 510 (2010).
[14] J.S. Netto, C.J.H. Cavalcanti and F. Ostermann, Revista Brasileira de Pesquisa em Educação em Ciências **19**, 1 (2019).
[15] F. Ostermann, C.J.H. Cavalcanti, S.D. Prado and T.F. Ricci, Revista Electrónica de Enseñanza de las Ciencias **8**, 1094 (2009).
[16] F. Ostermann and S.D. Prado, Revista Brasileira de Ensino de Física **27**, 193 (2005).
[17] F. Ostermann, S.D. Prado and T.F. Ricci, Física na Escola **7**, 22 (2006).
[18] A.P. Pereira, F. Ostermann and C.J.H. Cavalcanti, Physics Education **44**, 281 (2009).
[19] A.P. Pereira, F. Ostermann and C.J.H. Cavalcanti, Revista Electrónica de Enseñanza de las Ciencias **8**, 376 (2009).
[20] A.P. Pereira, O. Pessoa Jr., C.J.H. Cavalcanti and F. Ostermann, Caderno Brasileiro de Ensino de Física **29**, 831 (2012).
[21] T.F. Ricci, F. Ostermann and S.D. Prado, Revista Brasileira de Ensino de Física **29**, 79 (2007).
[22] J.S. Neto, F. Ostermann and S.D. Prado, Revista Brasileira de Ensino de Física **33**, 1401 (2011).
[23] J.S. Netto, C.J.H. Cavalcanti and F. Ostermann, Revista Brasileira de Pesquisa em Educação em Ciências **15**, 293 (2015).
[24] J.S. Netto, F. Ostermann and C.J.H. Cavalcanti, Caderno Brasileiro de Ensino de Física **35**, 185 (2018).
[25] N. Rutten, W.R. van Joolingen and J.T. van der Veen, Computers & Education **58**, 136 (2012).
[26] B. Berit, B.M. Vetleseter and H.E. Karoline, Science Education **102**, 856 (2018).
[27] P. Nachman, American Journal of Physics **63**, 39 (1995).
[28] K.P. Zetie, S.F. Adams and R.M. Tocknell, Physics Education **35**, 46 (2000).
[29] M.W. Hamilton, American Journal of Physics **68**, 186 (2000).
[30] R.L. Pfleegor and L. Mandel, Physics Letters A **24**, 766 (1967).
[31] P. Grangier, G. Roger and A. Aspect, Europhysics Letters **1**, 173 (1986).
[32] H.J. Snijders, J.A. Frey, J. Norman, H. Flayac, V. Savona, A.C. Gossard, J.E. Bowers, M.P. van Exter, D. Bouwmeester and W. Löffler, Physical Review Letters **121**, 043601 (2018).
[33] S. Tolansky, Physics Education **1**, 79 (1966).
[34] E. Hecht, *Optics* (Addison Wesley, San Francisco, 2002), 698 p.
[35] M.L.L. Iannini, Revista Brasileira de Ensino de Física **34**, 3309 (2012).
[36] P.A.M. Dirac, *The Principles of Quantum Mechanics* (Clarendon Press, Oxford, 1958).
[37] M. Michelini, R. Ragazzon, L. Santi and A. Stefanel, Physics Education **35**, 406 (2000).
[38] G. Auletta, S.Y. Wang and P. Pan Stanford, *Quantum Mechanics for Thinkers* (Pan Stanford Publishing, Singapore, 2014).
[39] G. Auletta, M. Fortunato and G. Parisi, *Quantum Mechanics* (Cambridge University Press, New York, 2014).
[40] M. Jammer, *The Philosophy of Quantum Mechanics: the Interpretations of Quantum Mechanics in Historical Perspective* (Wiley, New York, 1974).
[41] X. Peng, X. Zhu, D. Suter, J. Du, M. Liu and K. Gao, Physical Review A **72**, 052109 (2005).
[42] P.D.D. Schwindt, P.G. Kwiat and B.G. Englert, Physical Review A **60**, 4285 (1999).
[43] A. Danan, D. Farfurnik, S. Bar-Ad and L. Vaidman, Physical Review Letters **111**, 240402 (2013).
[44] Q. Duprey and A. Matzkin, Physical Review A **95**, 032110 (2017).
[45] B.G. Englert, K. Horia, J. Dai, Y.L. Len and H.K. Ng, Physical Review A **96**, 022126 (2017).
[46] P.L. Saldanha, Physical Review A **89**, 033825 (2014).
[47] D. Sokolovski, Physics Letters A **381**, 227 (2017).
[48] L. Vaidman, Physical Review A **87**, 052104 (2013).
[49] P.G. Kwiat, in: *Compendium of Quantum Physics*, edited by D. Greenberger, K. Hentschel and F. Weinert (Springer, Heidelberg, 2009), p. 428-434.
[50] V. Scarani and A. Suarez, American Journal of Physics **66**, 718 (1998).
[51] C.N. Villars, Physics Education **21**, 232 (1986).
[52] V. Degiorgio, American Journal of Physics **48**, 81 (1980).
[53] C.H. Holbrow, E. Galvez and M.E. Parks, American Journal of Physics **70**, 260 (2002).
[54] A. Luis and L.L. Sanchez-Soto, Quantum and Semiclassical Optics: Journal of the European Optical Society Part B **7**, 153 (1995).
[55] A. Zeilinger, American Journal of Physics **49**, 882 (1981).
[56] R. Omnès, Reviews of Modern Physics **64**, 339 (1992).
[57] D.C. Giancoli, *Physics: Principles with Applications* (Pearson Education, New Jersey, 2005), 946 p.
[58] G. Auletta, *Foundations and Interpretation of Quantum Mechanics: in the Light of a Critical-Historical Analysis of the Problems and of a Synthesis of the Results* (World Scientific, Singapore, 2001).
[59] V. Scarani, *Quantum Physics, a First Encounter: Interference, Entanglement, and Reality* (Oxford University Press, Oxford, 2006).
[60] W. Wootters and W. Zurek, Physical Review D **19**, 473 (1979).
[61] D.M. Greenberger and A. Yasin, Physics Letters A **128**, 391 (1988).
[62] G. Jaeger, A. Shimony and L. Vaidman, Physical Review A **51**, 54 (1995).
[63] B.G. Englert, Physical Review Letters **77**, 2154 (1996).

[64] M.N. Bera, T. Qureshi, M.A. Siddiqui and A.K. Pati, Physical Review A **92**, 012118 (2015).
[65] T. Qureshi, American Journal of Physics **84**, 517 (2016).
[66] S. Dürr, T. Nonn and G. Rempe, Physical Review Letters **81**, 5705 (1998).
[67] L. Li, N.L. Liu and S. Yu, Physical Review A **85**, 054101 (2012).
[68] V. Jacques, E. Wu, F. Grosshans, F. Treussart, P. Grangier, A. Aspect and J.F. Roch, Physical Review Letters **100**, 220402 (2008).
[69] A. Luis and I. Gonzalo, European Journal of Physics **36**, 025012 (2015).
[70] A. Maries, R. Sayer and C. Singh, Physical Review Physics Education Research **13**, 020115 (2017).
[71] D.J. Griffiths, *Introduction to Quantum Mechanics* (Pearson Prentice Hall, New Jersey, 2004), 480 p.
[72] R.A. Serway and J.W. Jewett, *Principles of Physics: a Calculus-Based Text* (Cengage Learning, Melbourne, 2013), 1192p.
[73] P.A. Tipler and R.A. Llewellyn, *Modern Physics* (Macmillan Higher Education, New York, 2012).
[74] H.D. Young and R.A. Freedman, *University Physics with Modern Physics* (Addison-Wesley, San Francisco, 2012), 1598 p.
[75] C.W. Helstrom, *Quantum Detection and Estimation Theory* (Academic Press, New York, 1976).
[76] J.A. Bergou, U. Herzog and M. Hillery, in: *Quantum State Estimation*, edited by M. Paris and J. Řeháček (Springer, Heidelberg, 2004), p. 417-465.
[77] T. Dittrich, European Journal of Physics **36**, 1 (2015).
[78] C.E. Shannon, The Bell System Technical Journal **27**, 379 (1948).
[79] L. Benguigui, European Journal of Physics **34**, 303 (2013).
[80] R.K. Pathria and P.D. Beale, *Statistical Mechanics* (Elsevier, Amsterdam, 2011).
[81] J.R.H. Tame, *Approaches to Entropy* (Springer, Singapore, 2019).
[82] E.T. Jaynes, *Probability Theory* (Cambridge University Press, Cambridge, 2003).
[83] A. Zeilinger, Physica B+C **137**, 235 (1986).
[84] A. Chao and T.J. Shen, Environmental and Ecological Statistics **10**, 429 (2003).
[85] R.K. Sawyer and S. Berson, Linguistics and Education **15**, 387 (2004).
[86] D. Hicks, in: *Discourse, Learning, and Schooling*, edited by D. Hicks (Cambridge University Press, New York, 2008), p. 104-141.
[87] E. Marshman and C. Singh, Physical Review Physics Education Research **13**, 010117 (2017).